Overview of Radio Coronal Magnetography

OUTLINE (PART 1)

The uses and abuses of various emission mechanisms

- Thermal free-free radiation
- Thermal gyroresonance radiaton (SW)
- Nonthermal gyrosynchrotron radiation
- Radio bursts

OUTLINE (PART 2)

Propagation phenomena and related

- Ray tracing
- Scattering phenomena
- Faraday rotation
- QT propagation

THERMAL SUN AT RADIO WAVELENGTHS

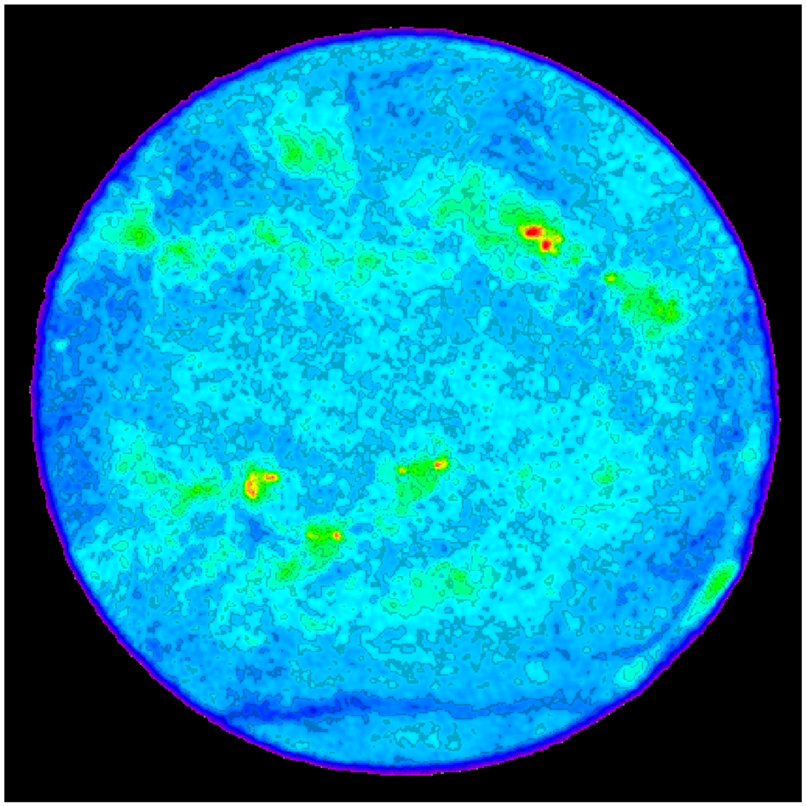

VLA: 4.9 GHz

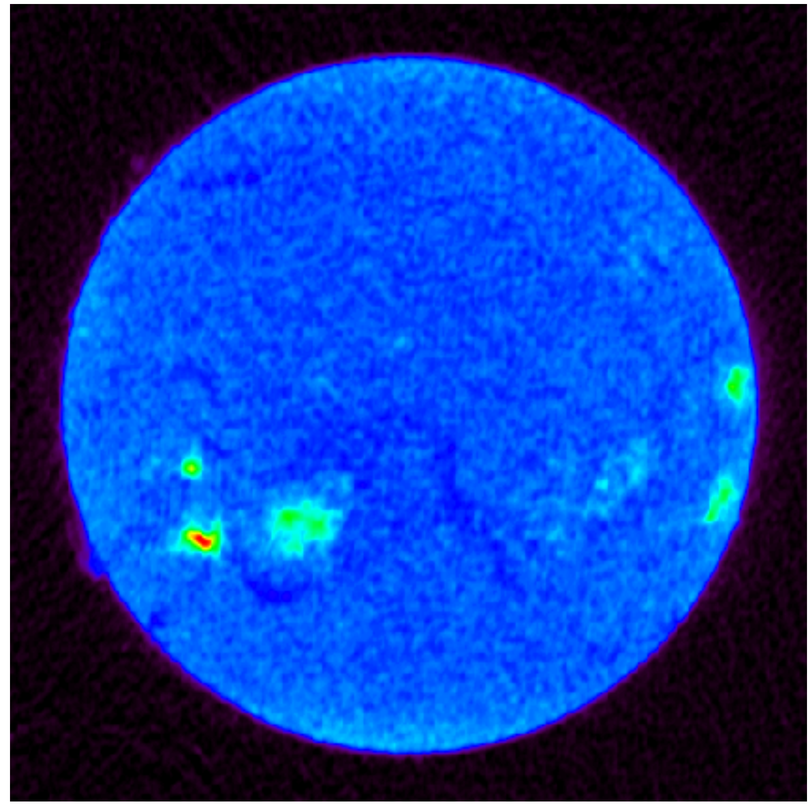

NoRH: 17 GHz

THERMAL SUN AT RADIO WAVELENGTHS

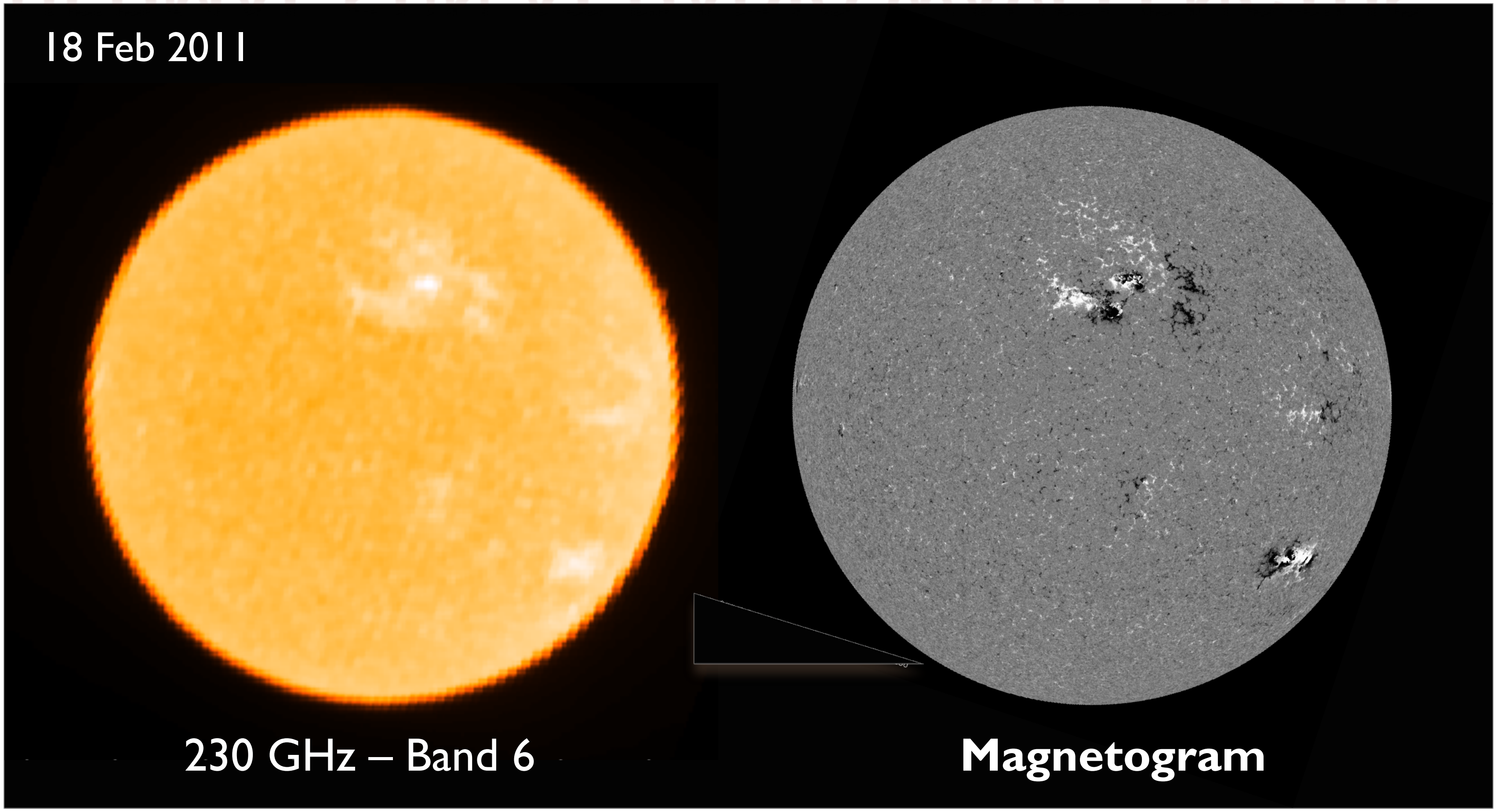

FREE-FREE ABSORPTION

- The two magnetoionic modes correspond to orthogonal circular polarizations ($\sigma=+1$ o-mode, $\sigma=-1$ x-mode)

$$\kappa_{R,L} = \left(\frac{2}{\pi}\right)^{1/2} \frac{1}{3c} \frac{\nu_p^2}{(\nu+\sigma\nu_B\cos\theta)^2} \frac{4\pi e^4 \sum_i Z_i^2 n_i}{m^{1/2}(kT)^{3/2}} \Lambda(T,\nu)$$

$$\approx 0.2 n^2 T^{-3/2} \nu^{-2} (1 \mp \sigma 2 \frac{\nu_{Be}}{\nu} \cos\theta)$$

- Free-free emission favors low frequencies, low temperatures, high number densities
- The brightness temperature spectrum of optically thin emission is flat (ignoring the Gaunt factor)
- Polarization $\rho_c = (T_R - T_L)/(T_R + T_L) \approx 2(\nu_{BE}/\nu)\,|\cos\theta| \quad (\tau << 1)$

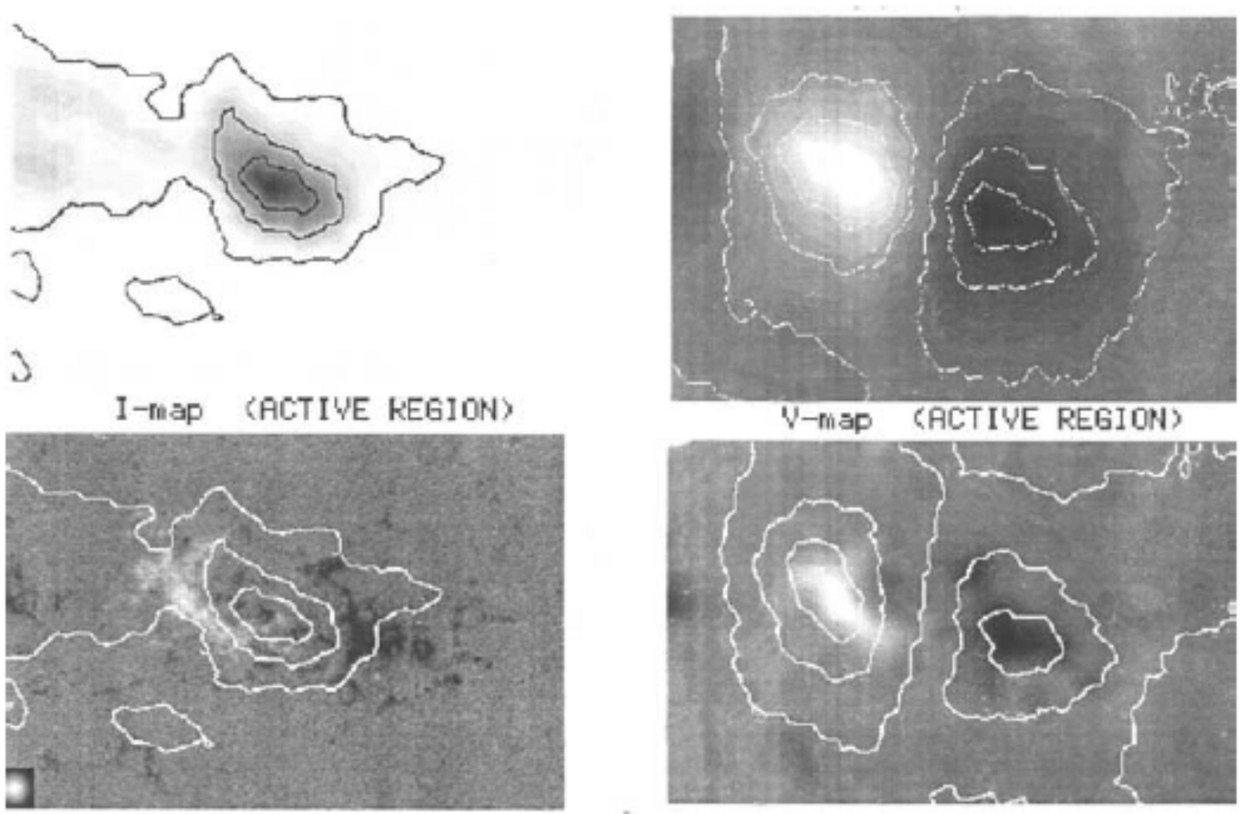

B~85 G

Figure 5.1. Radio maps of the AR observed on June 09, 1995 using Nobeyama radio heliograph at $\lambda = 1.76cm$. Contours present the brightness distribution . Maximum in I channel ($T_b = 27 \cdot 10^3 K$). Maximum in V-channel $T_b^V = 440K$. Maximum degree of polarization $P = 2.8\%$. The region maps are overlapped by gray scale magnetograms . For V-maps they are averaged by the scale of the Nobeyama radio heliograph beam (shown below on the left). The upper V-map present brightness T_b^V, the lower one - percentage $P\%$ of polarization.

Gelfreikh 2003

Another example

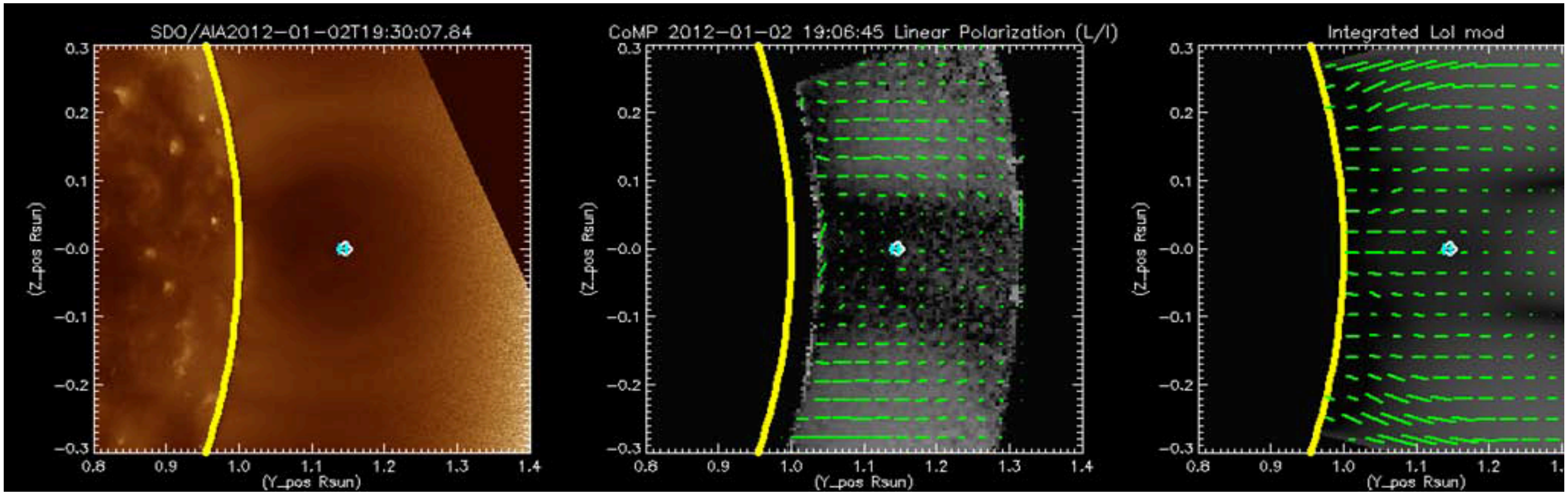

Joint VLA/CoMP observations of a coronal cavity on the disk and at the limb.

For VLA: observations across the 1-2 GHz band, dual-pol'n, 1024 channels.

$$\rho_C = V / I \approx 0.6\% B_{los} / \nu_9 \qquad\qquad T_V \approx 240 L_{10} B_{los} / \nu_9^3$$

Complementary to CoMP IR measurements of POS linearly polarized emission.

FREE-FREE EMISSION

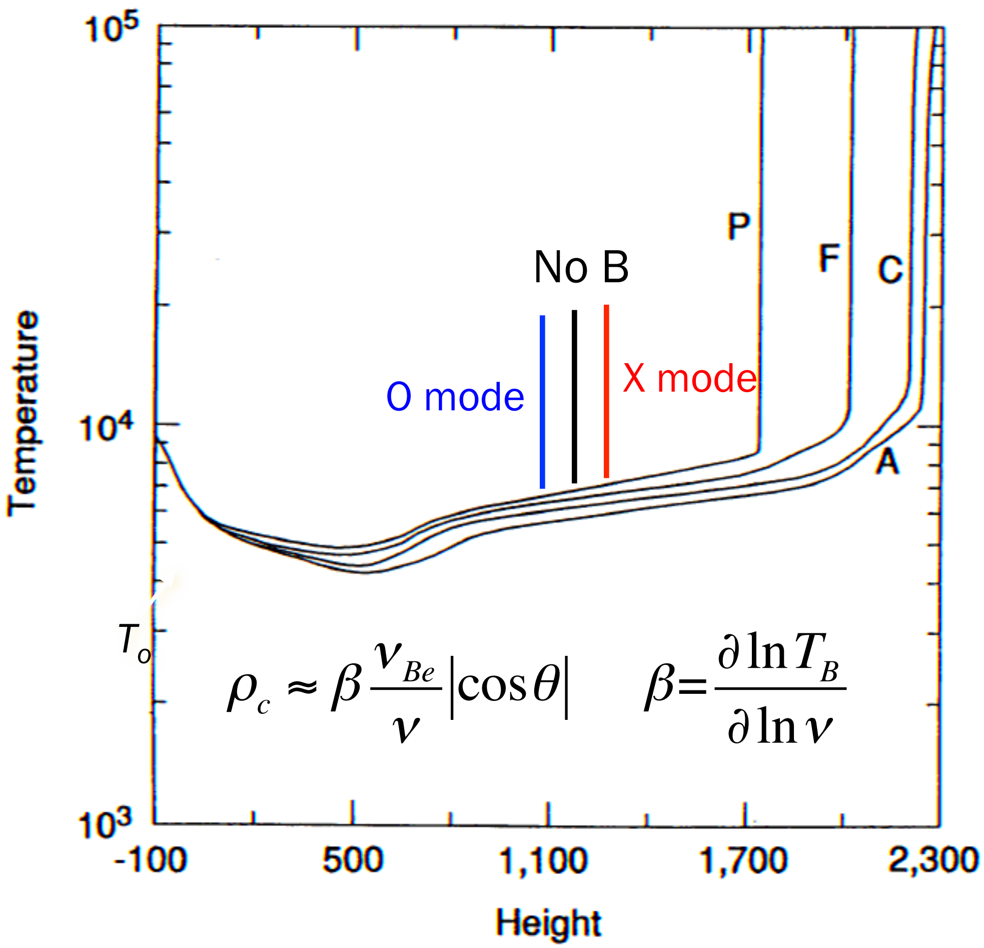

FIG. 3.—Temperature structure of our models A, C, F, and P. The height is measured in kilometers from the level; the temperature is in kelvins.

Optically thick case

- With no magnetic field, both modes have same opacity & reach $\tau = 1$ at same height and hence, no polarized emission.
- Even with $|B| > 0$, no polarized emission unless temperture gradients are present.
- If so, x-mode becomes optically thick slightly higher in the chromosphere & has a higher brightness temperature.
- O-mode is optically thick at slightly lower temperature.
- Non-zero pol'n provides magnetic field signature.

Fontenla, Avrett & Loeser (1993)

Free-Free Emission

Strengths:

✓ubiquitous

✓can be used to constrain fields of any strength ($\nu >> \nu_{B\varepsilon}$)

✓both optically thin and optically thick emission can be exploited

✓technique can be employed on the disk or the limb

Weaknesses/complications:

✓provides measure of longitudinal component of B only

✓optically thin measure is a weighted line of sight integral through the medium (sensitive to T_e, n_e, B_l)

✓limited angular resolution

STANDARD MODEL

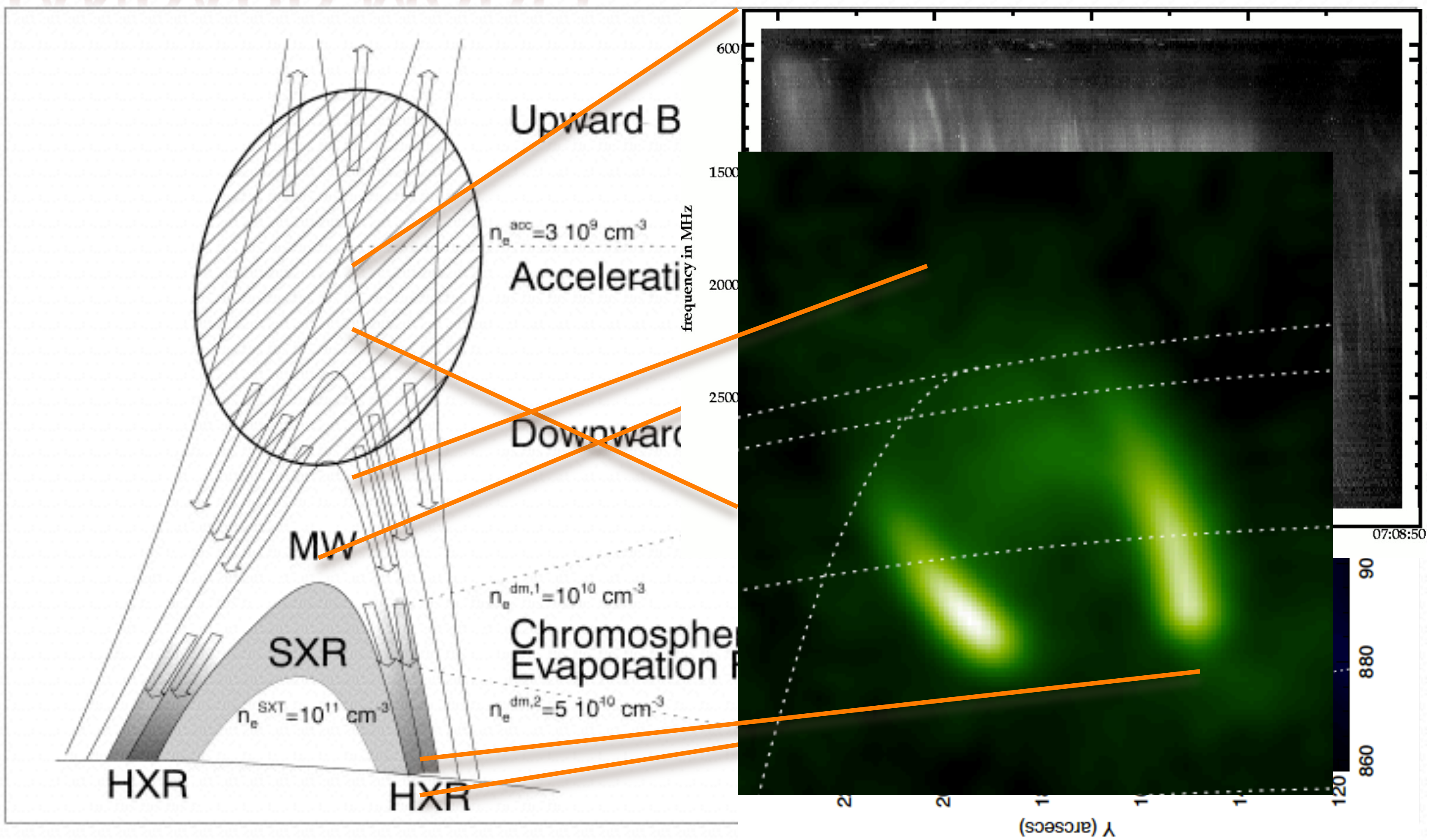

Aschwanden & Benz 1997

13 July 2005 LDE: 0230-0500 UT

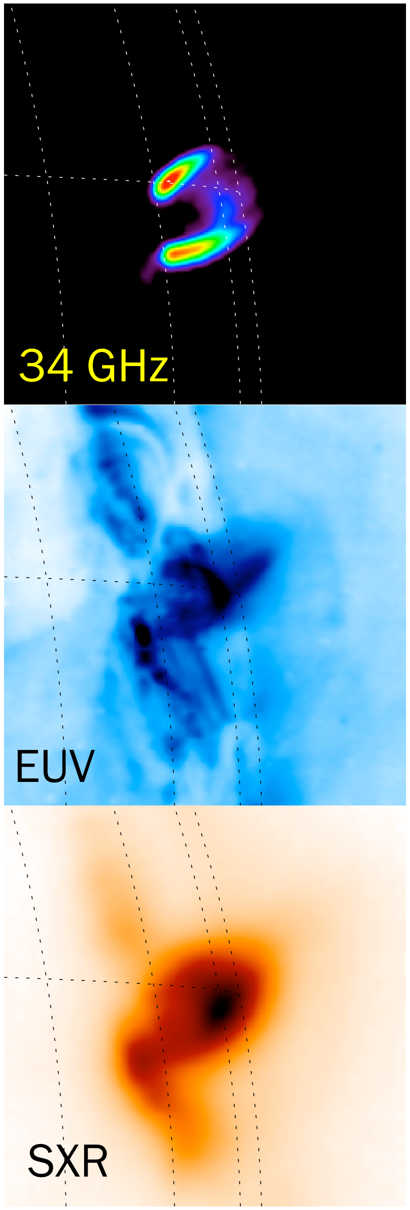

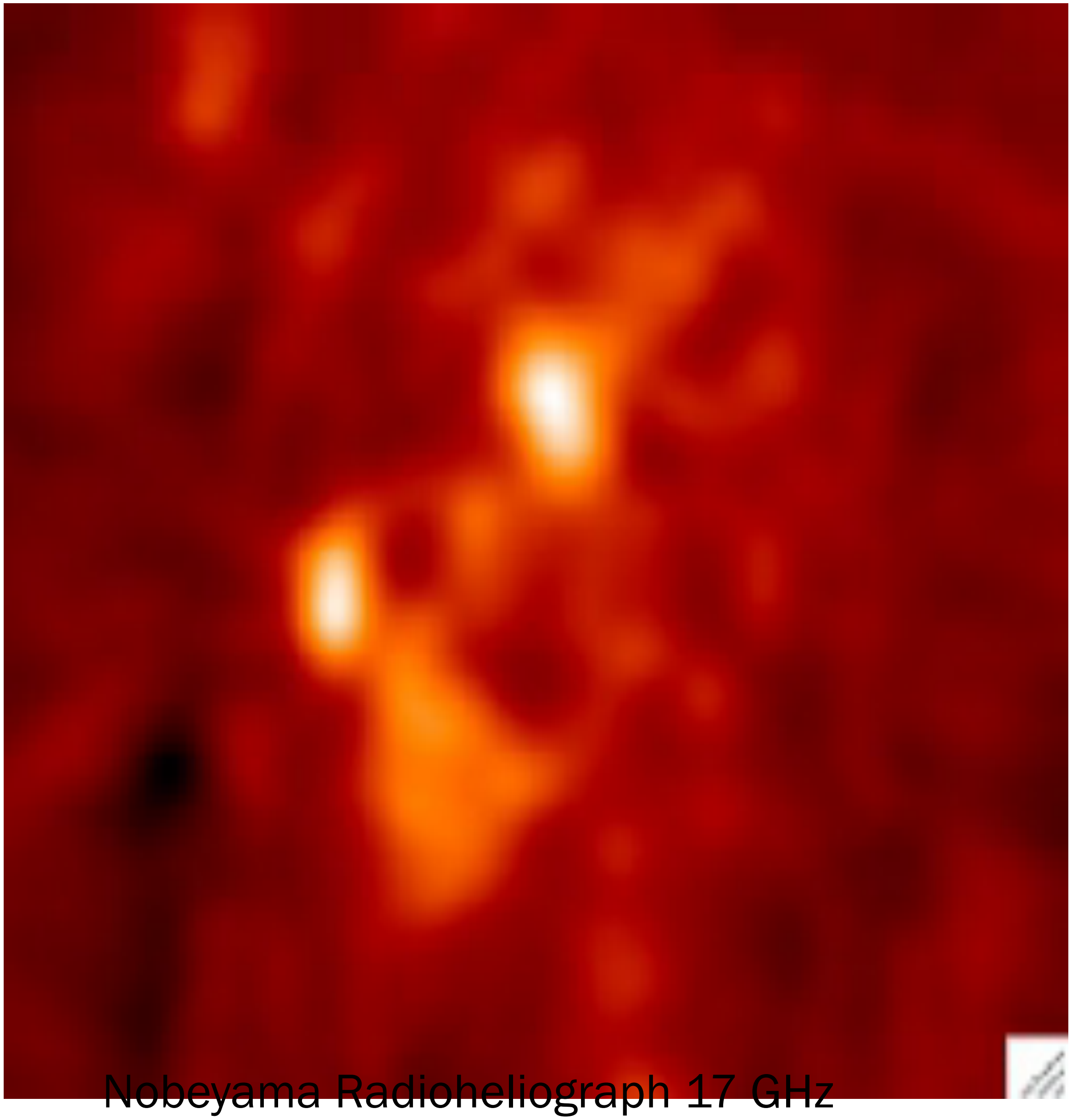

Nobeyama Radioheliograph 17 GHz

1992 June 26

Joint OVSA/BATSE observations of a C7.2 flare

Spectral slope inferred from HXR a good match to the (optically thin) footpoint microwave spectrum only.

Conditions in loop top appeared different from those in footpoint.

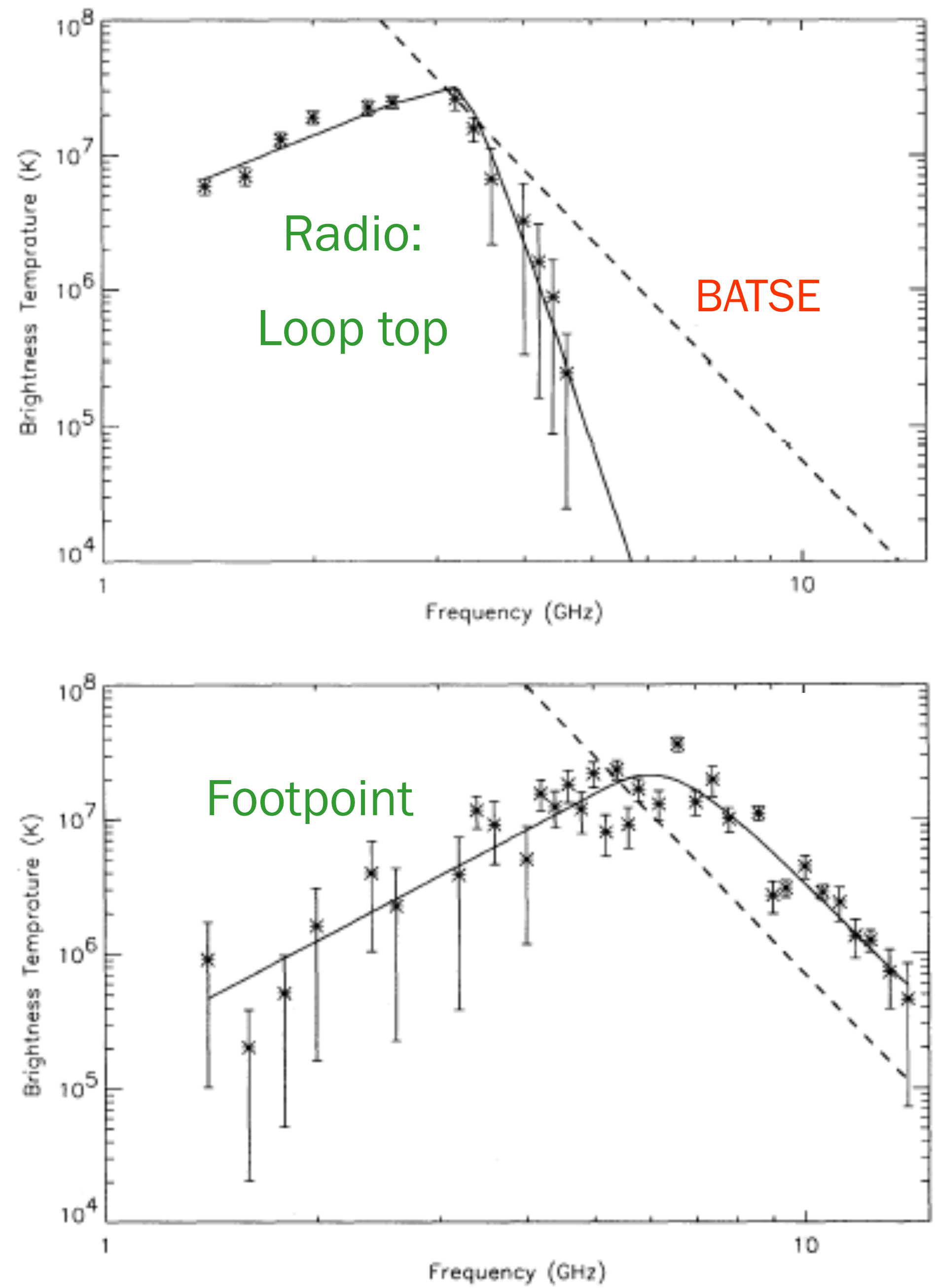

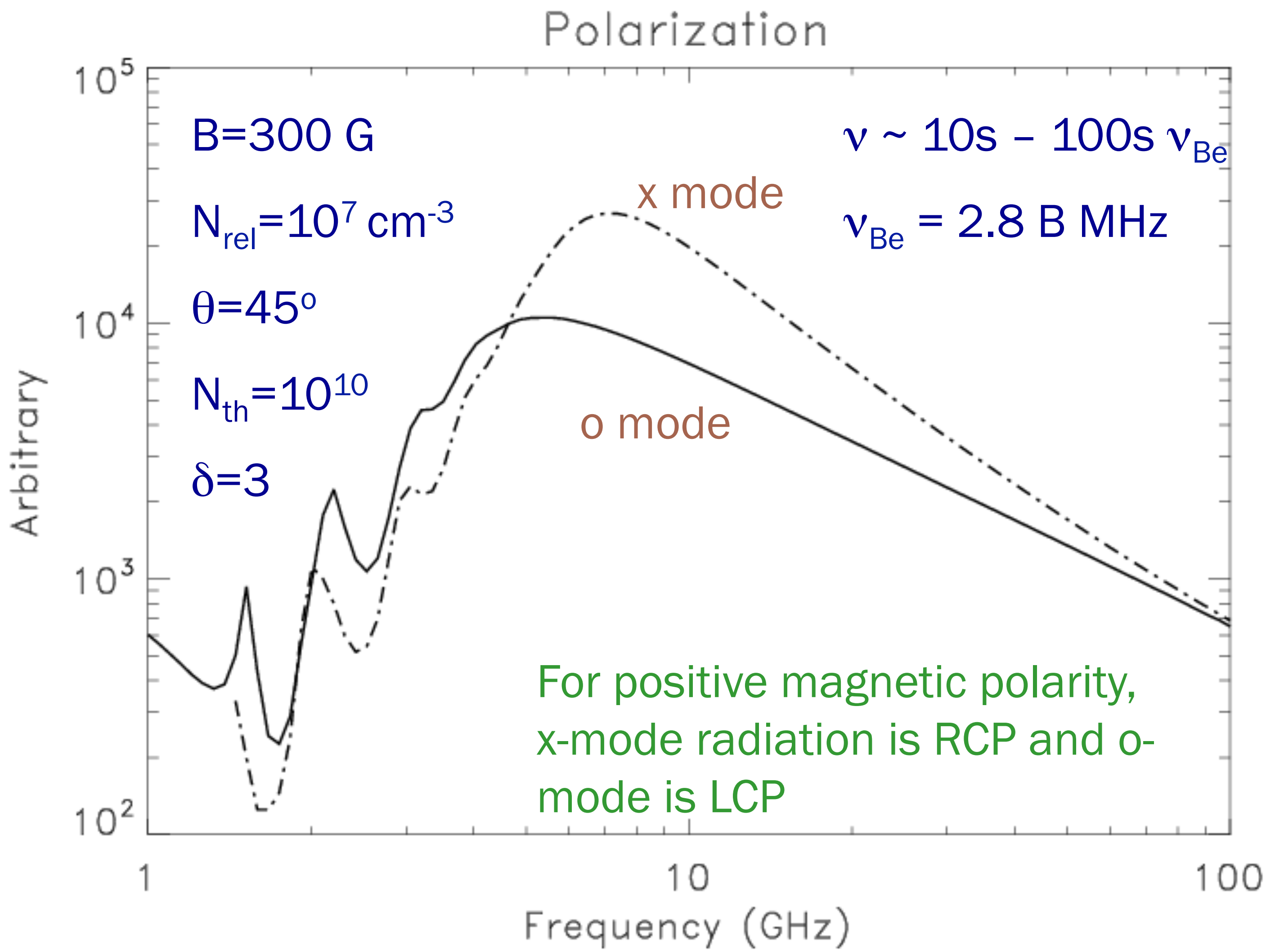
Polarization
B=300 G
$N_{rel}=10^7$ cm^{-3}
$\theta=45^o$
$N_{th}=10^{10}$
$\delta=3$
ν ~ 10s – 100s ν_{Be}
ν_{Be} = 2.8 B MHz
x mode
o mode
For positive magnetic polarity, x-mode radiation is RCP and o-mode is LCP
Arbitrary
Frequency (GHz)
10^5
10^4
10^3
10^2
1
10
100

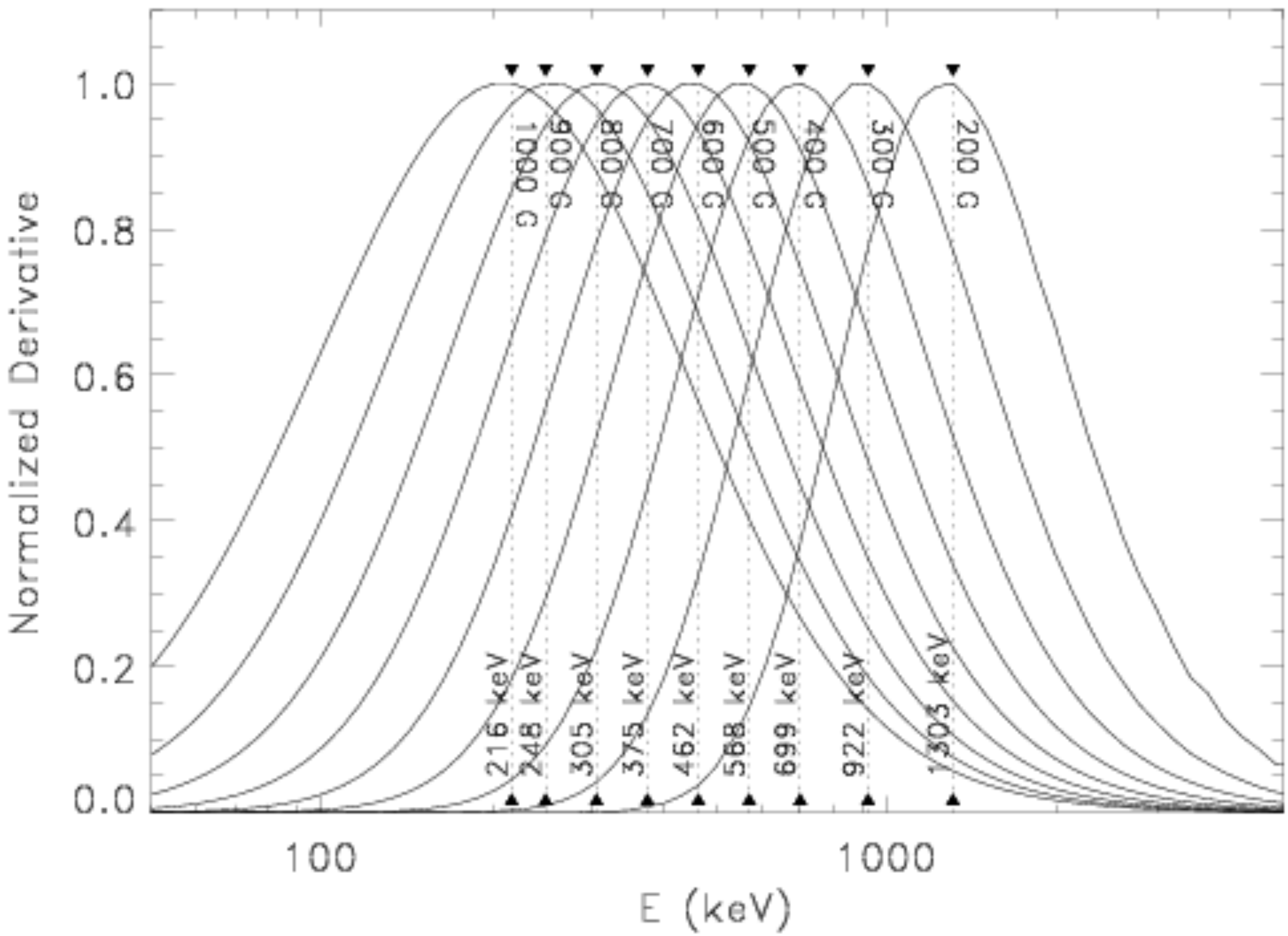

Normalized Derivative
E (keV)
1000 G
900 G
800 G
700 G
600 G
500 G
400 G
300 G
200 G
216 keV
248 keV
305 keV
375 keV
462 keV
588 keV
699 keV
922 keV
1303 keV

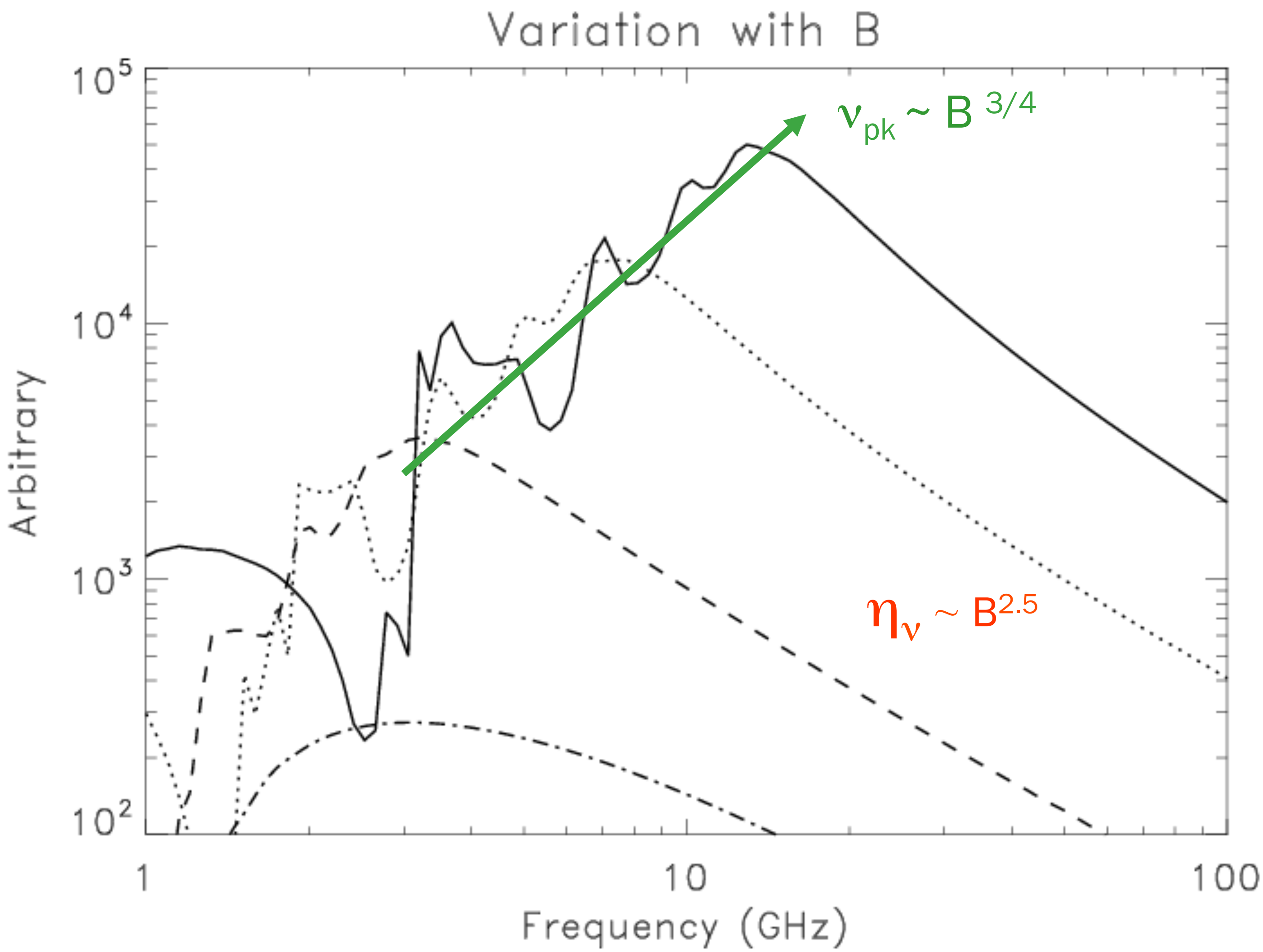
Variation with B
$\nu_{pk} \sim B^{3/4}$
$\eta_\nu \sim B^{2.5}$
Arbitrary
Frequency (GHz)
10^5
10^4
10^3
10^2
1
10
100

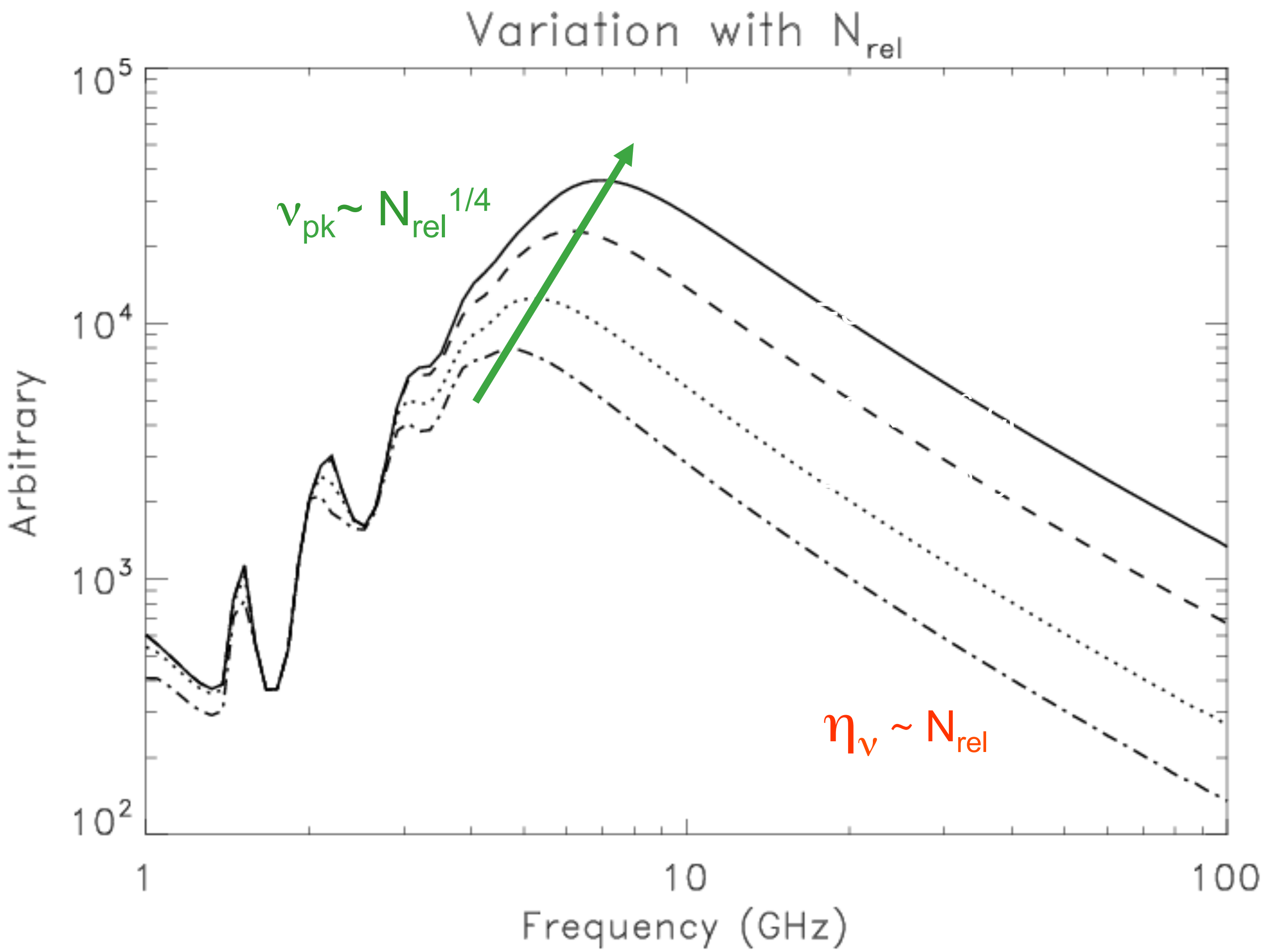

Variation with N_rel
10^5
10^4
10^3
10^2
Arbitrary
1
10
100
Frequency (GHz)
ν_pk ~ N_rel^1/4
η_ν ~ N_rel

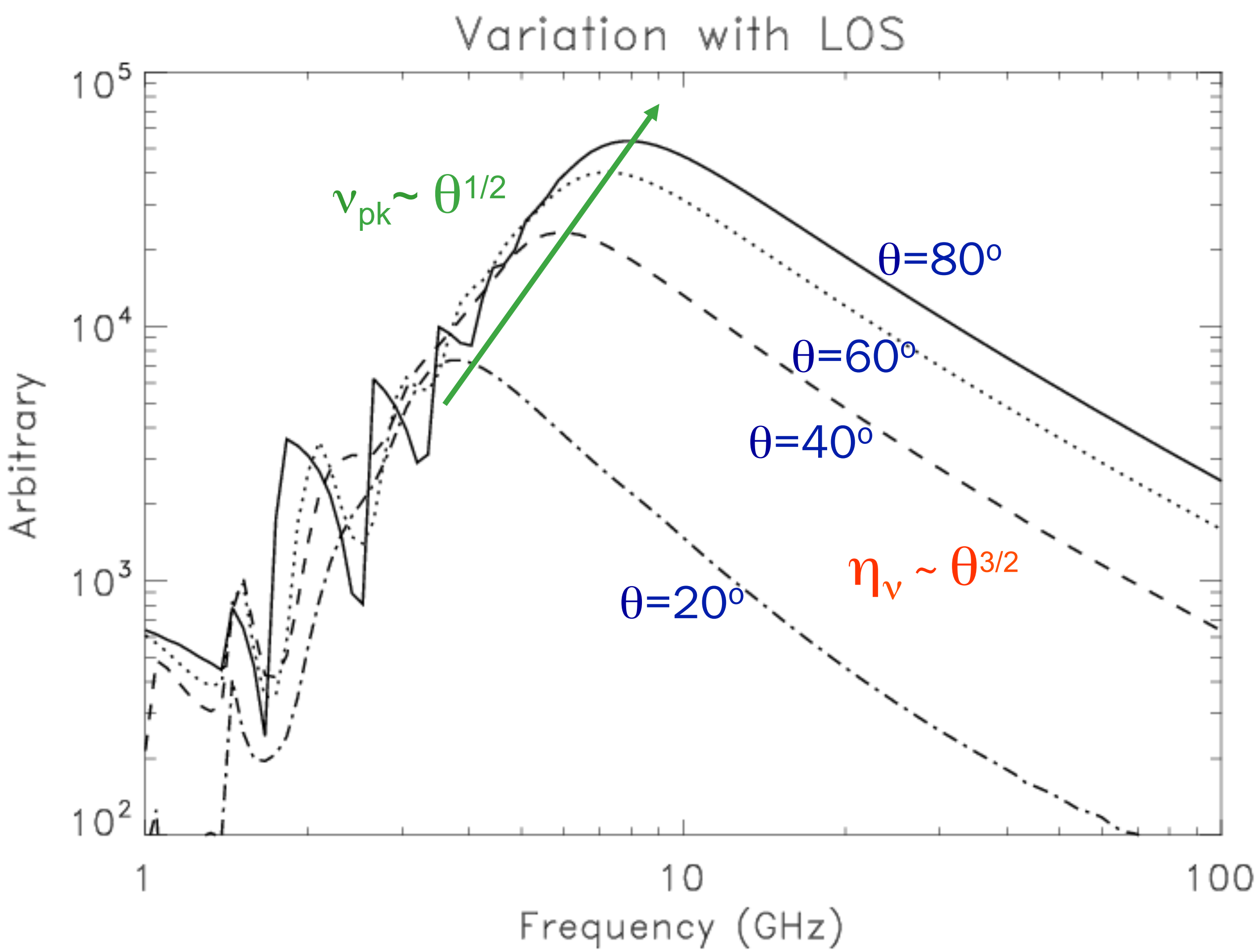
Variation with LOS
10^5
10^4
10^3
10^2
Arbitrary
1
10
100
Frequency (GHz)
ν_pk ~ θ^1/2
θ=80°
θ=60°
θ=40°
θ=20°
η_ν ~ θ^3/2

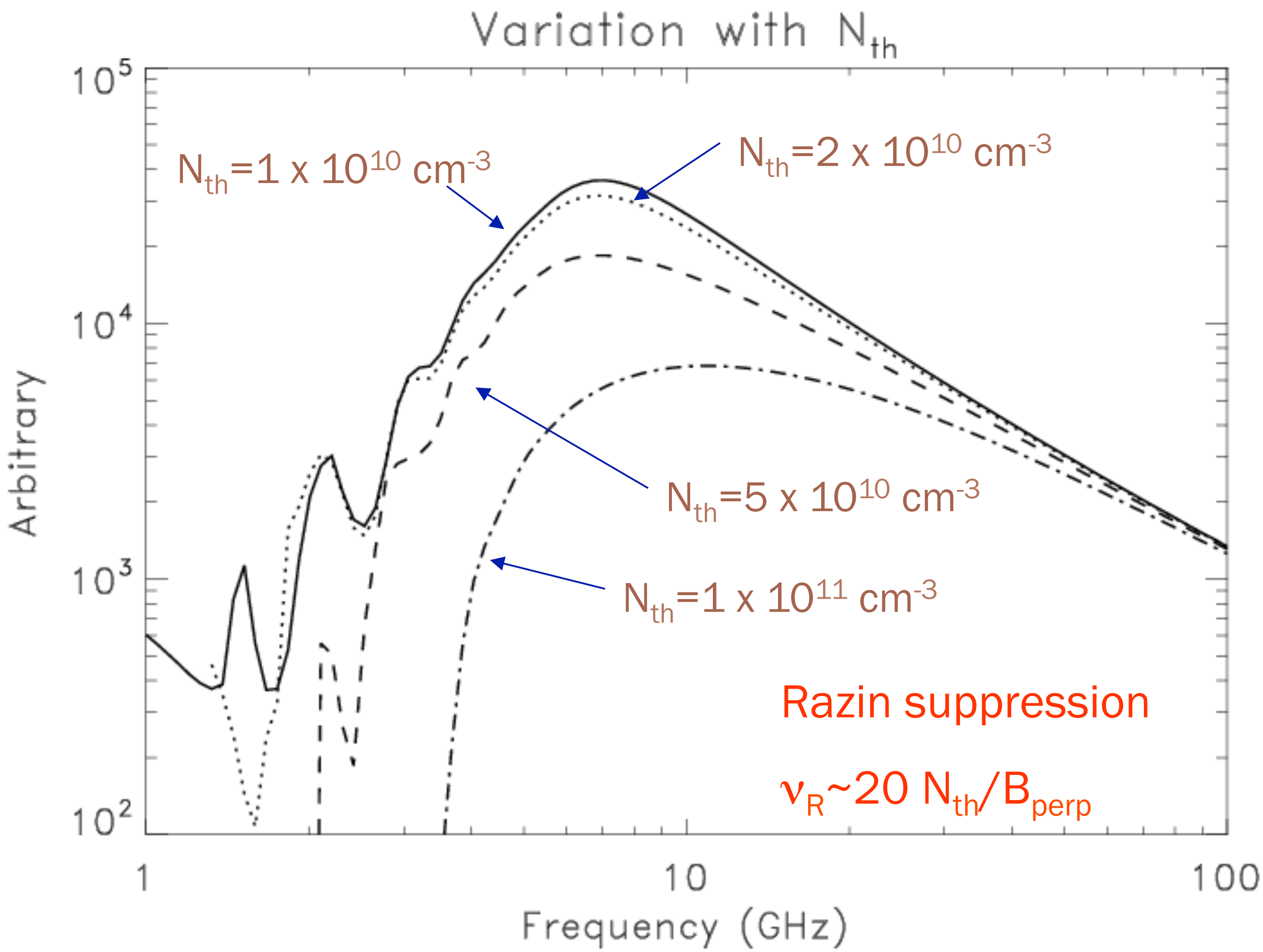

Variation with N_th
10^5
10^4
10^3
10^2
Arbitrary
1
10
100
Frequency (GHz)
N_th=1 x 10^10 cm^-3
N_th=2 x 10^10 cm^-3
N_th=5 x 10^10 cm^-3
N_th=1 x 10^11 cm^-3
Razin suppression
ν_R~20 N_th/B_perp

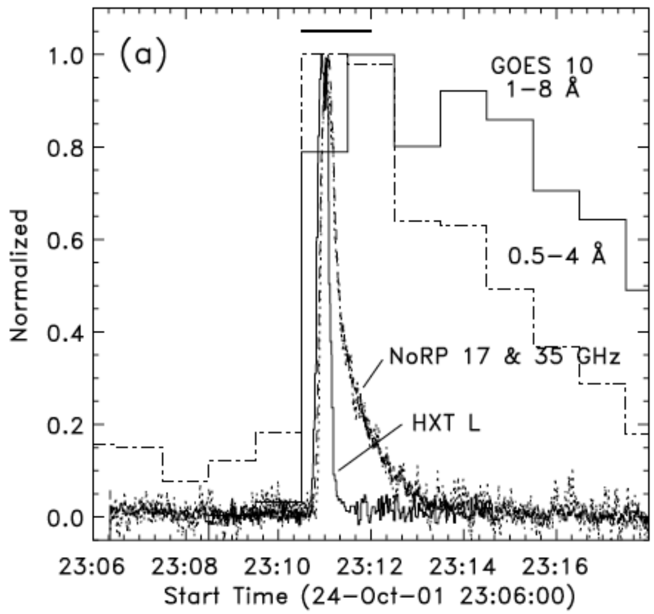
(a)
GOES 10
1–8 Å
0.5–4 Å
NoRP 17 & 35 GHz
HXT L
Normalized
1.0
0.8
0.6
0.4
0.2
0.0
23:06
23:08
23:10
23:12
23:14
23:16
Start Time (24–Oct–01 23:06:00)

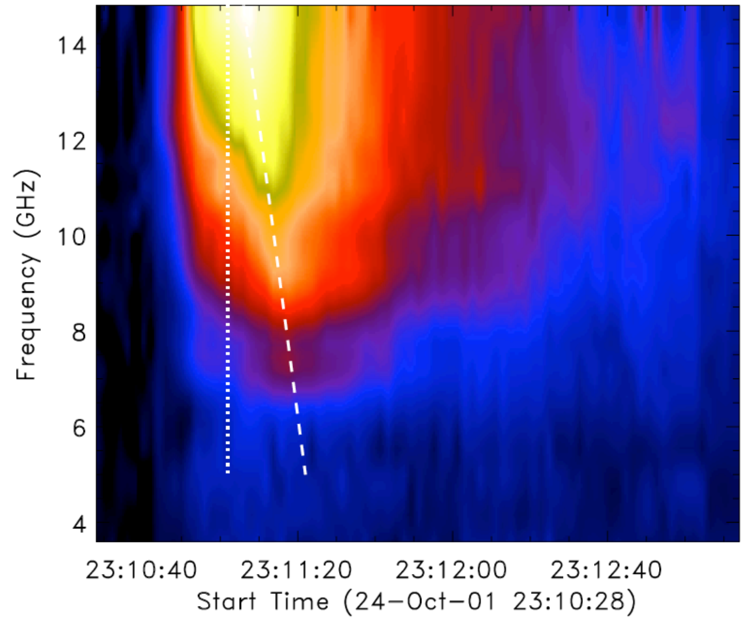
Frequency (GHz)
14
12
10
8
6
4
23:10:40
23:11:20
23:12:00
23:12:40
Start Time (24–Oct–01 23:10:28)

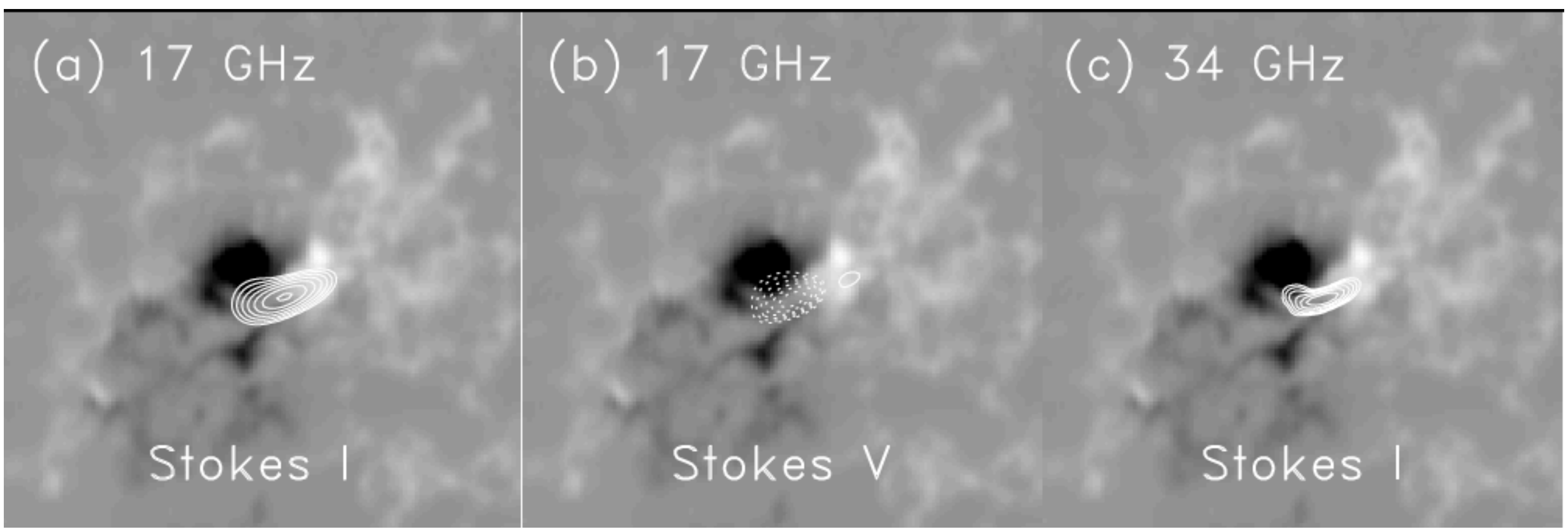
(a) 17 GHz
Stokes I
(b) 17 GHz
Stokes V
(c) 34 GHz
Stokes I

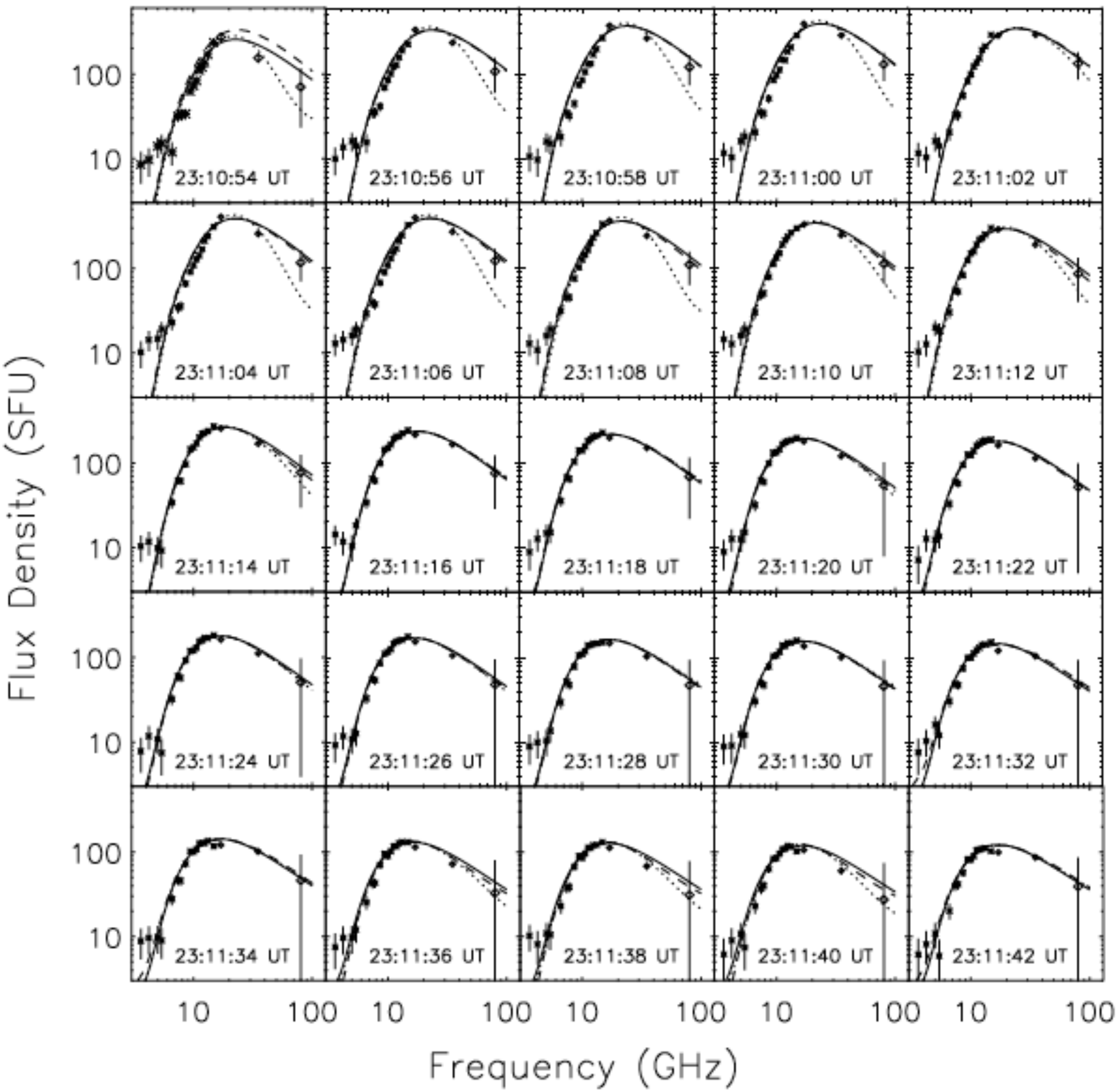
Flux Density (SFU)
Frequency (GHz)
23:10:54 UT
23:10:56 UT
23:10:58 UT
23:11:00 UT
23:11:02 UT
23:11:04 UT
23:11:06 UT
23:11:08 UT
23:11:10 UT
23:11:12 UT
23:11:14 UT
23:11:16 UT
23:11:18 UT
23:11:20 UT
23:11:22 UT
23:11:24 UT
23:11:26 UT
23:11:28 UT
23:11:30 UT
23:11:32 UT
23:11:34 UT
23:11:36 UT
23:11:38 UT
23:11:40 UT
23:11:42 UT

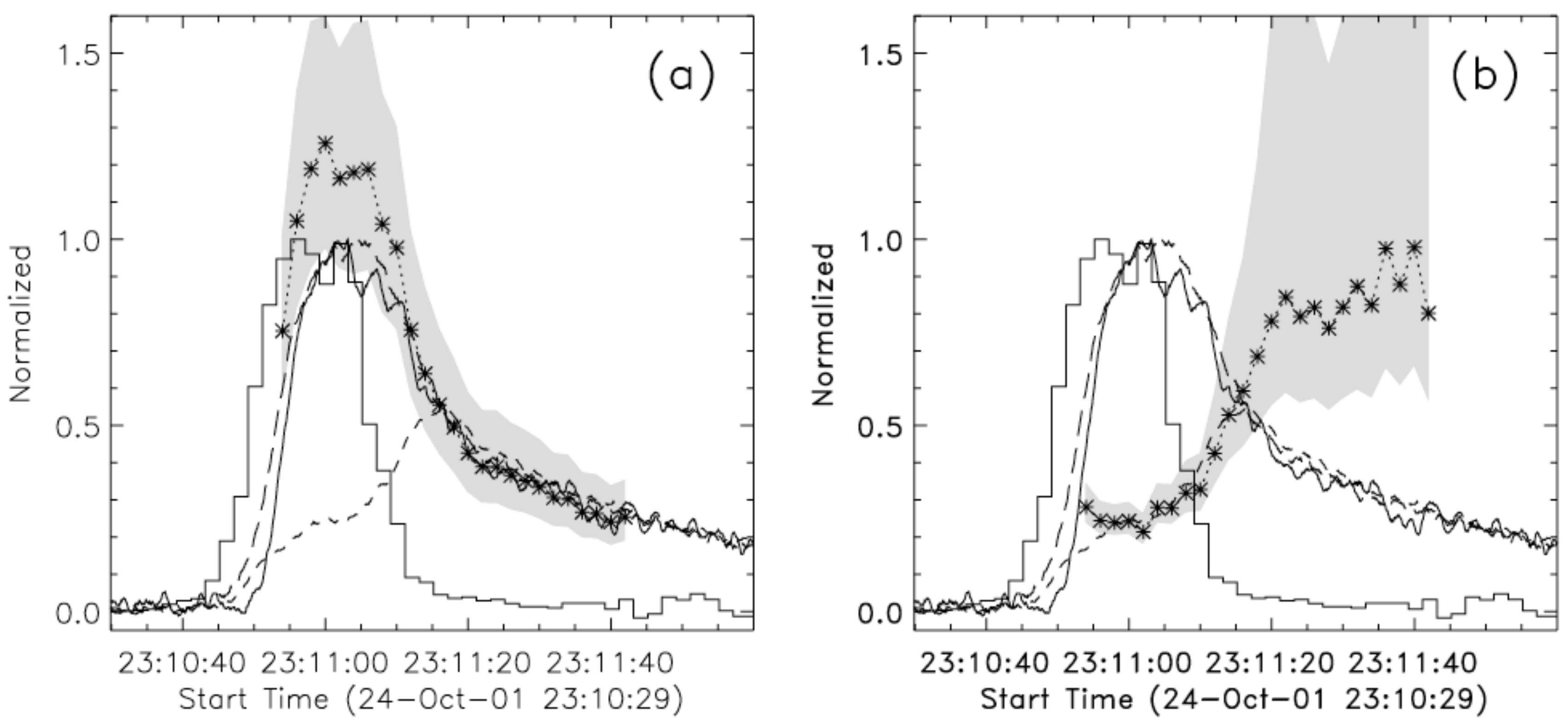
(a)
(b)
Normalized
0.0
0.5
1.0
1.5
23:10:40
23:11:00
23:11:20
23:11:40
Start Time (24-Oct-01 23:10:29)

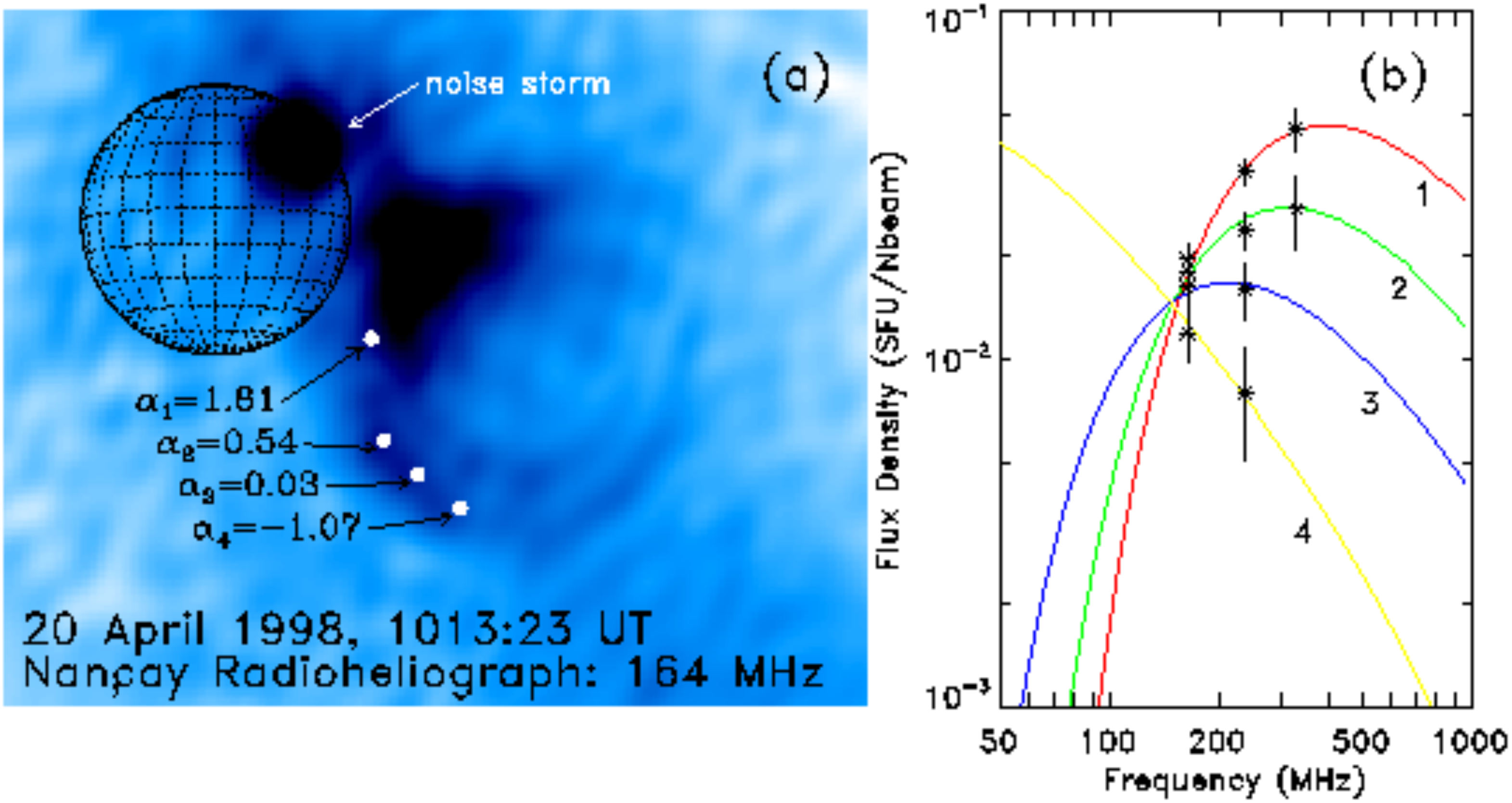

LoS	α	R_{sun}	ϕ (deg)	n_e (cm^{-3})	B(G)	ν_{RT} (MHz)
1	1.81	1.45	234	2.5×10^7	1.47	330
2	0.54	2.05	218.5	1.35×10^7	1.03	265
3	0.03	2.4	219.5	6.5×10^6	0.69	190
4	-1.07	2.8	221	5×10^5	0.33	30

Bastian et al. 2001

Detection of synchrotron radiation from MeV electrons interacting with magnetic field entrained by fast CME.

2001 April 15: X14.4 flare, partial halo CME >1200 km/s, major SEP event

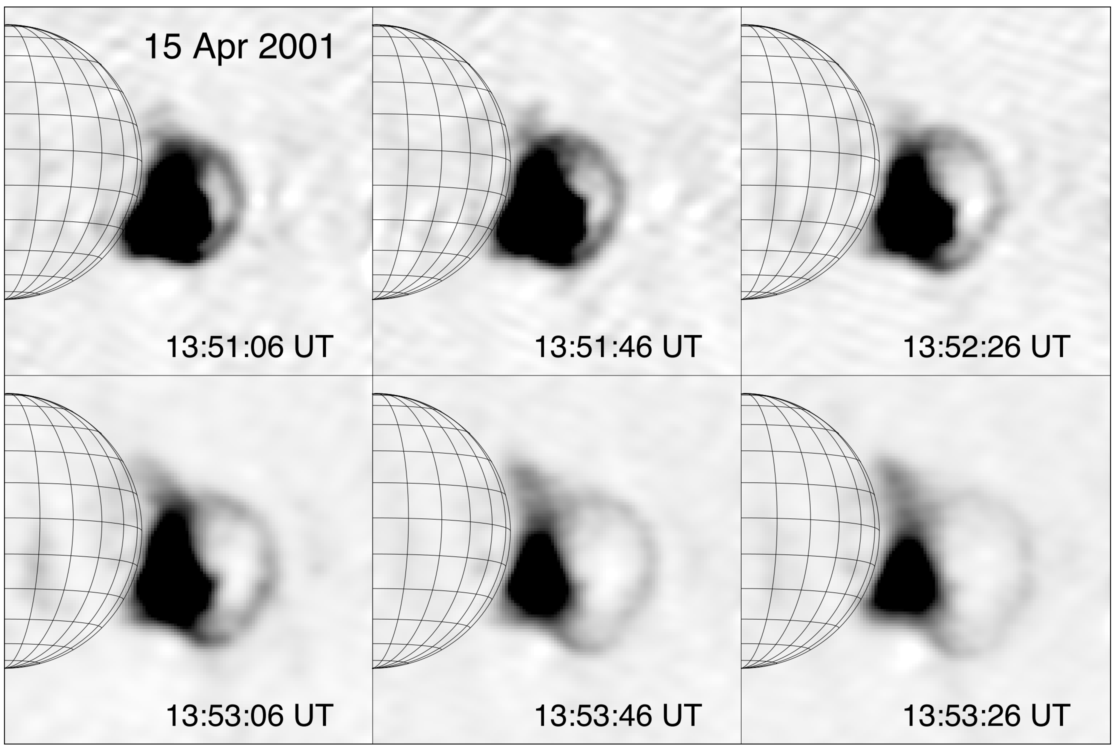

Nancay RH: 327 MHz

Maia et al. (2007)

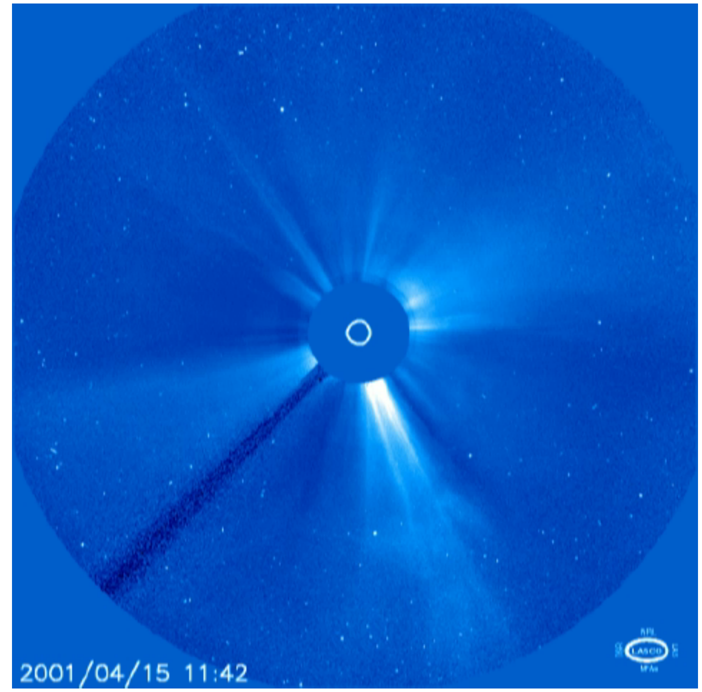

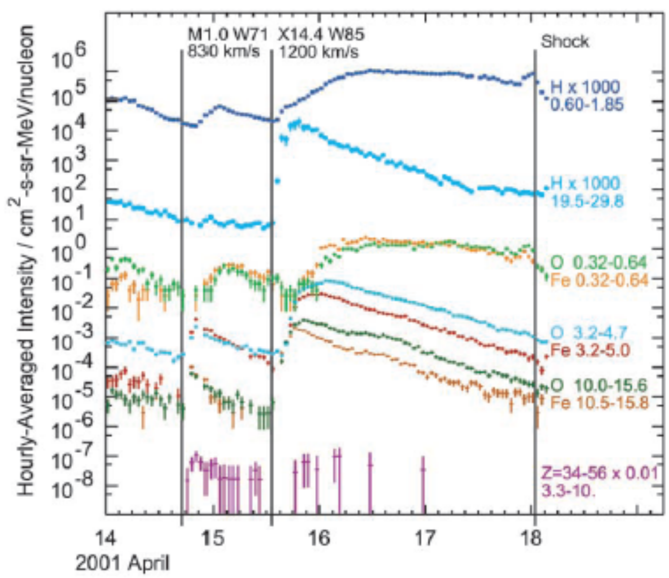

Tylka et al. (2002)

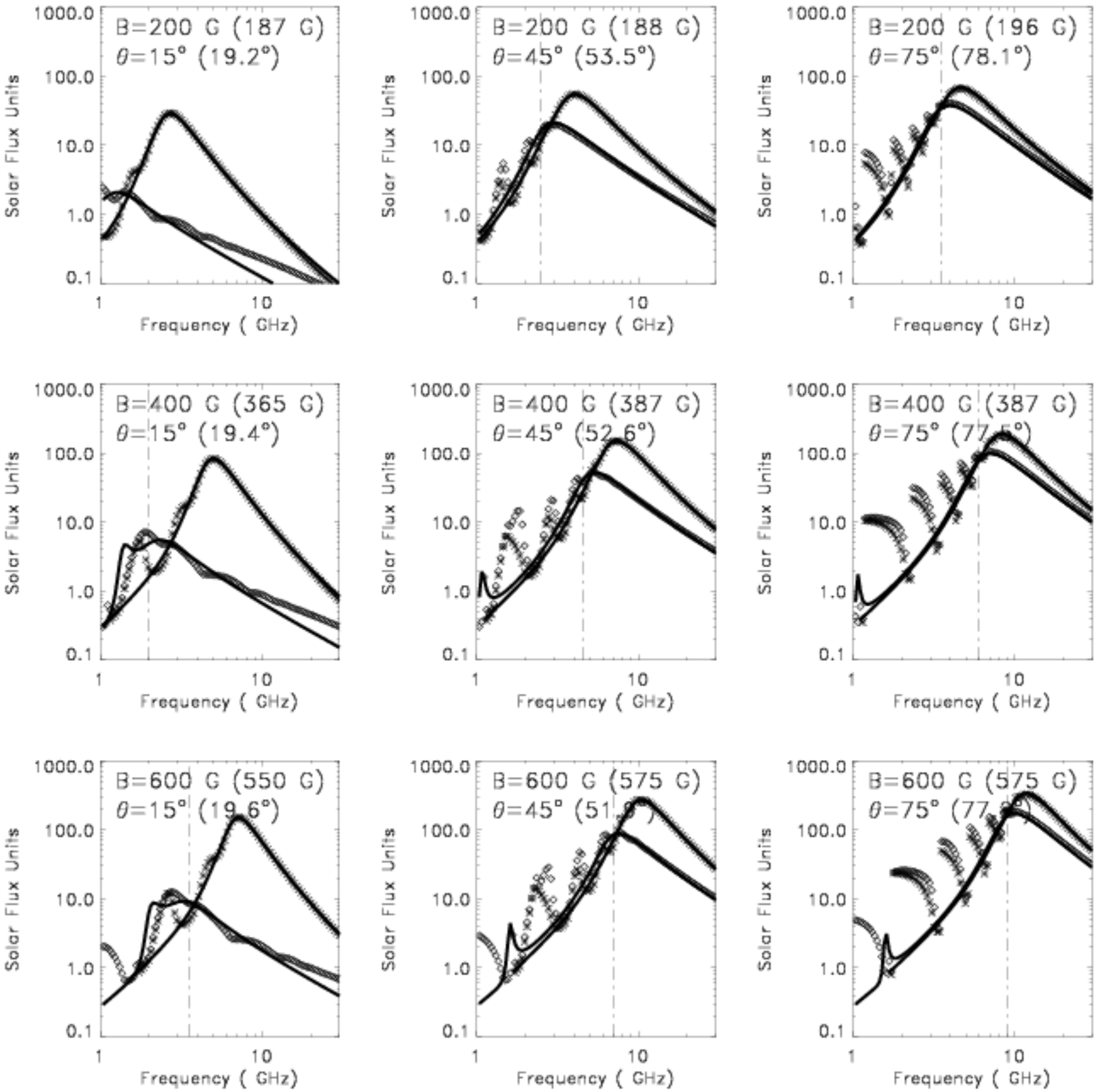

Coronal Magnetography via GSR Inversion

General method to invert both GR and GSR spectra.

Proceed via χ^2-minimization

Physics embodied in model in flexible manner

Much work needed to establish robust and efficient algorithms

Bastian 2005

Fast Spectral Inversion

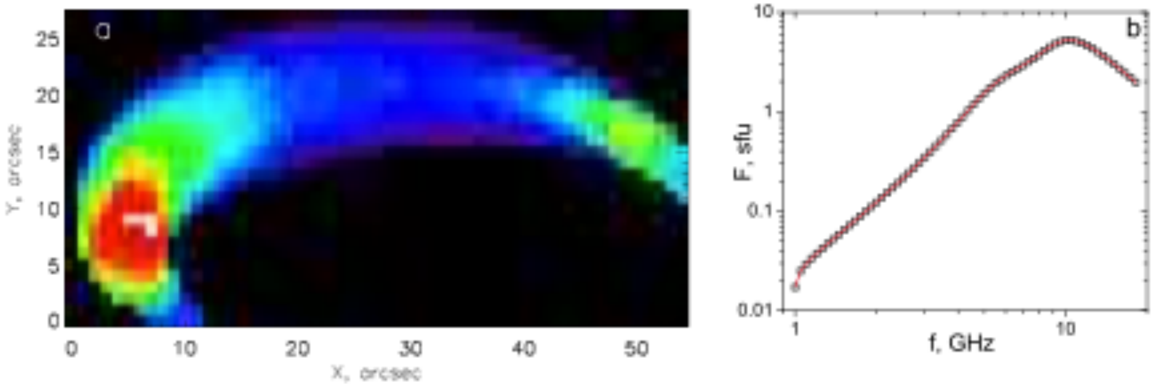

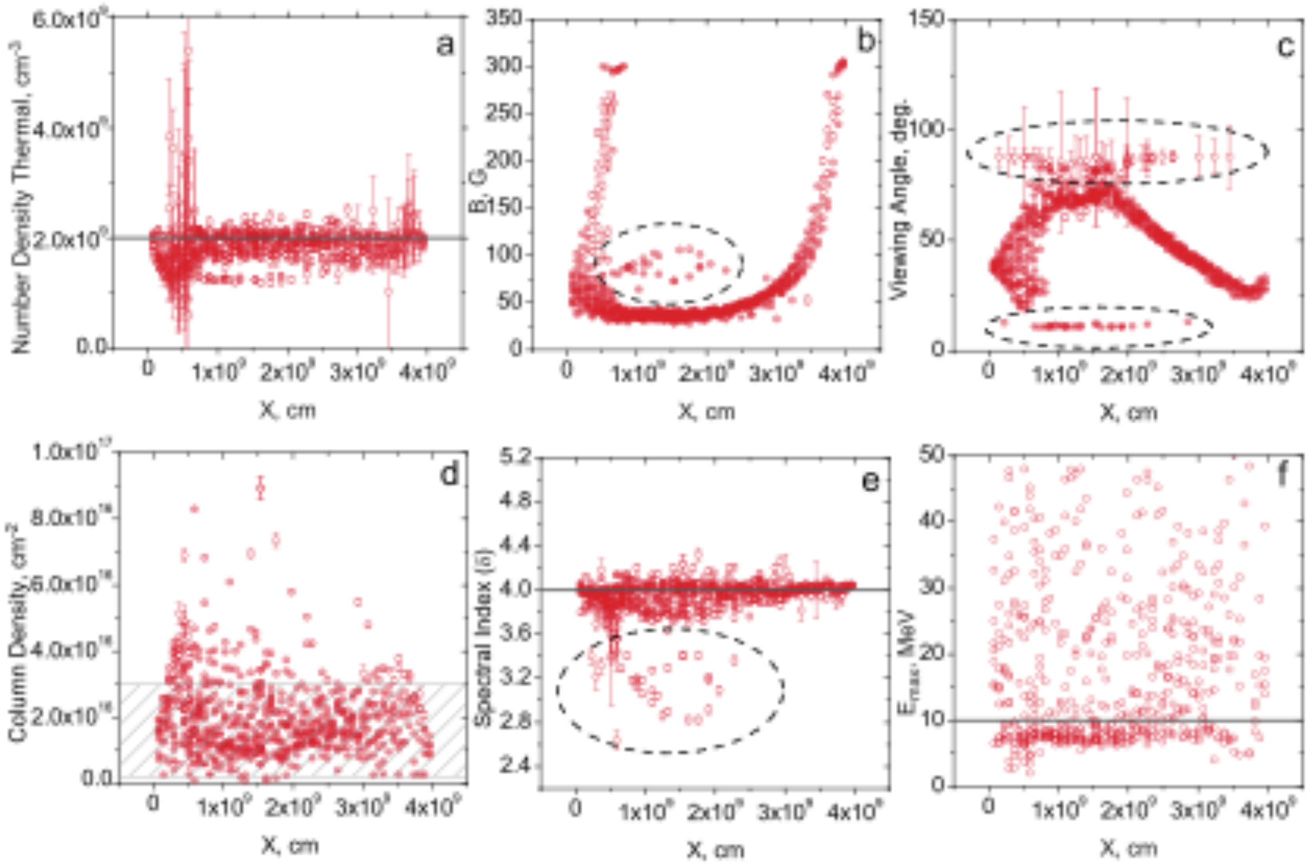

Fast gyrosynch. codes required!

Fleishman & Kuznetsov 2010

Fleishman et al. 2009

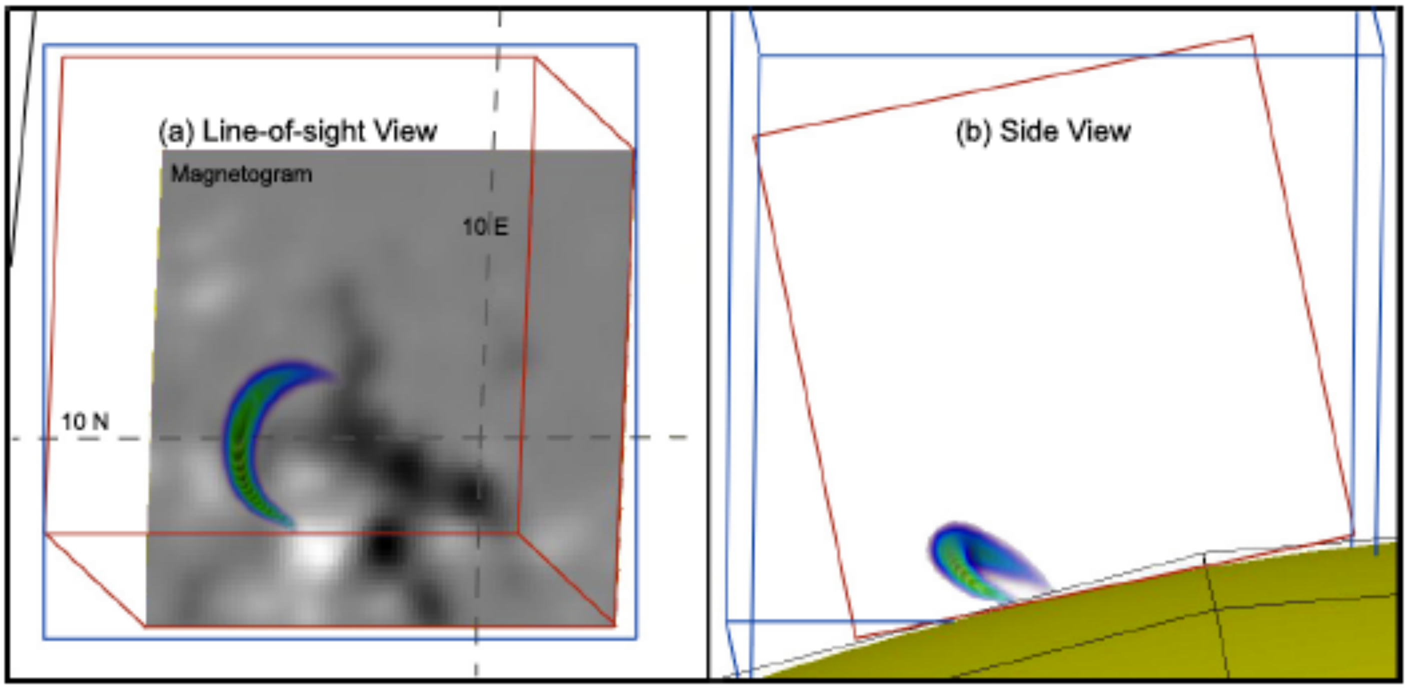

(a) Line-of-sight View
Magnetogram
10 E
10 N
(b) Side View

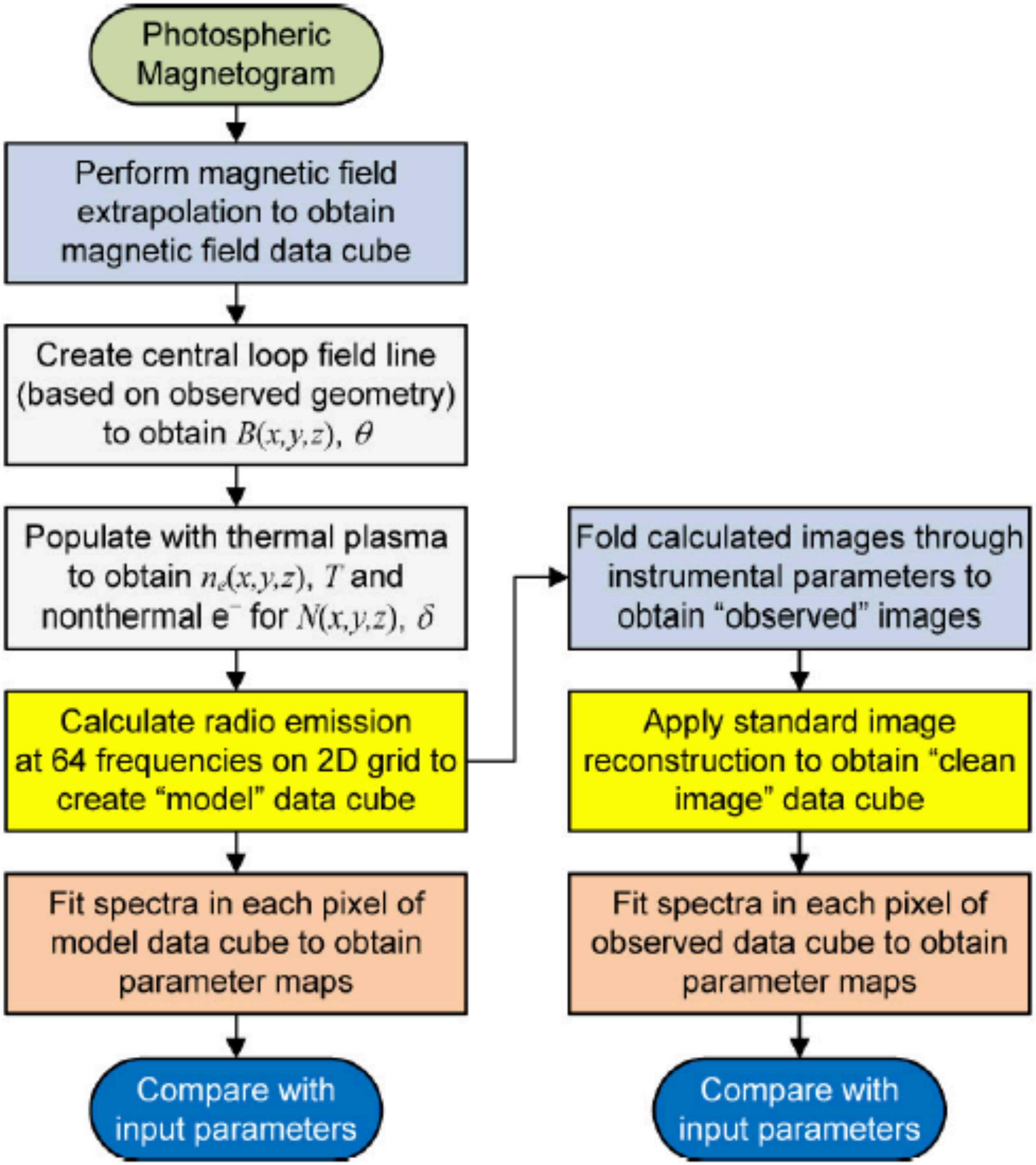

Photospheric Magnetogram
Perform magnetic field extrapolation to obtain magnetic field data cube
Create central loop field line (based on observed geometry) to obtain B(x,y,z), θ
Populate with thermal plasma to obtain n_e(x,y,z), T and nonthermal e⁻ for N(x,y,z), δ
Calculate radio emission at 64 frequencies on 2D grid to create "model" data cube
Fit spectra in each pixel of model data cube to obtain parameter maps
Compare with input parameters
Fold calculated images through instrumental parameters to obtain "observed" images
Apply standard image reconstruction to obtain "clean image" data cube
Fit spectra in each pixel of observed data cube to obtain parameter maps
Compare with input parameters

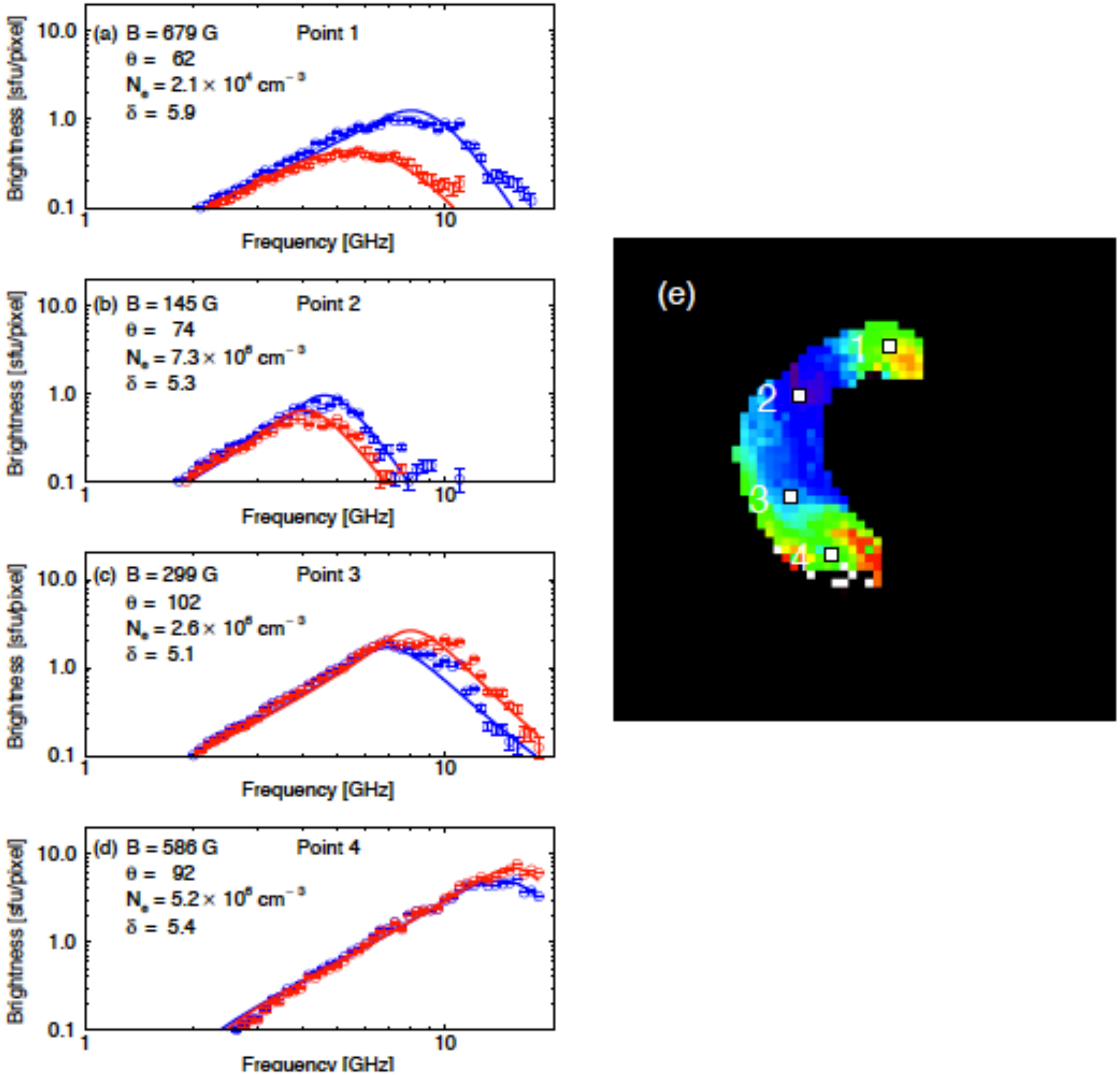

(a) B = 679 G
Point 1
θ = 62
N_e = 2.1 × 10^4 cm^-3
δ = 5.9
(b) B = 145 G
Point 2
θ = 74
δ = 5.3
(c) B = 299 G
Point 3
θ = 102
δ = 5.1
(d) B = 586 G
Point 4
θ = 92
δ = 5.4
Brightness [sfu/pixel]
Frequency [GHz]
10.0
1.0
0.1
1
10
(e)
1
2
3
4

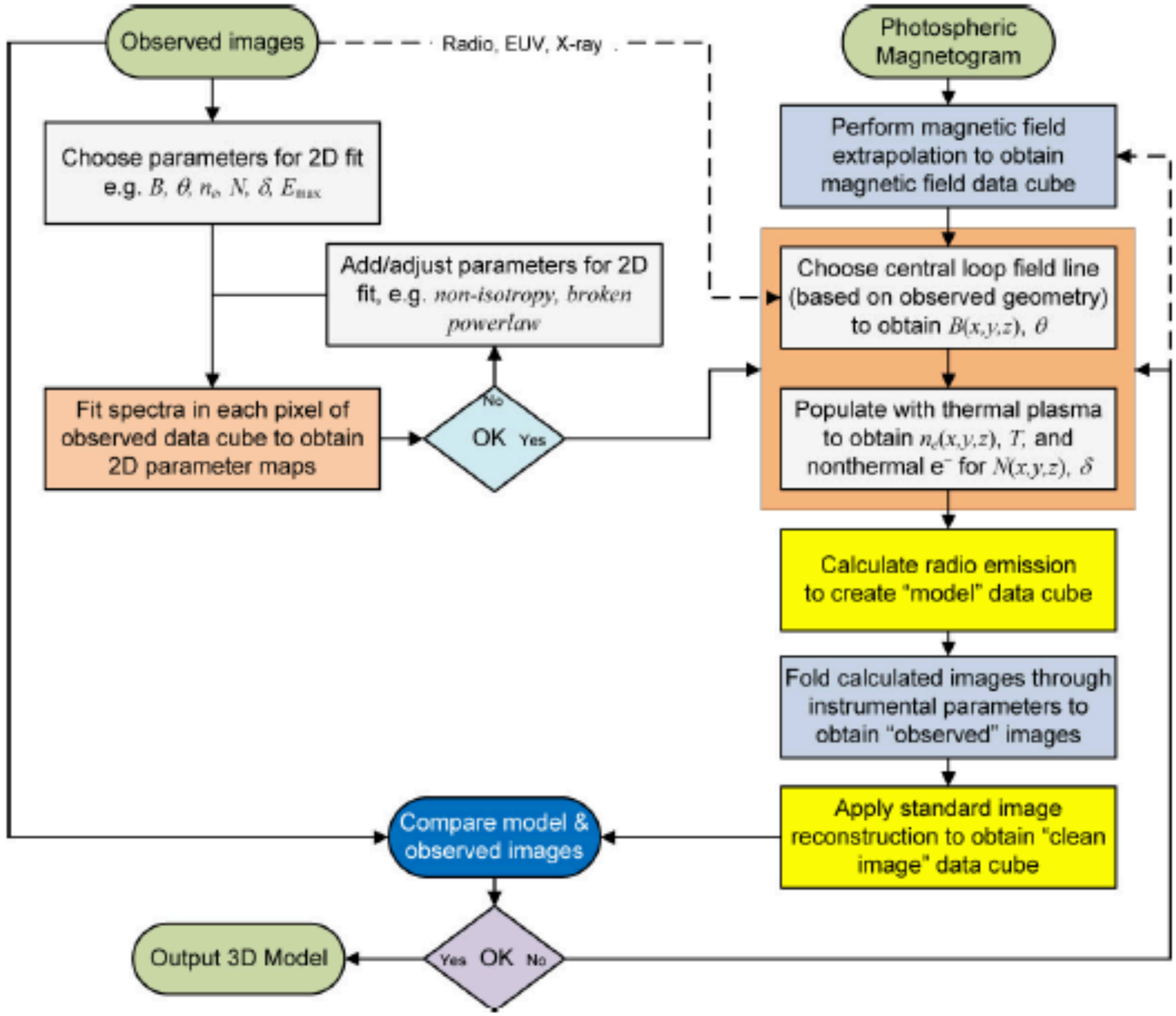

Observed images
Radio, EUV, X-ray
Photospheric Magnetogram
Choose parameters for 2D fit e.g. B, θ, n_e, N, δ, E_{max}
Perform magnetic field extrapolation to obtain magnetic field data cube
Add/adjust parameters for 2D fit, e.g. non-isotropy, broken powerlaw
Choose central loop field line (based on observed geometry) to obtain $B(x,y,z)$, θ
Fit spectra in each pixel of observed data cube to obtain 2D parameter maps
No
OK
Yes
Populate with thermal plasma to obtain $n_e(x,y,z)$, T, and nonthermal e⁻ for $N(x,y,z)$, δ
Calculate radio emission to create "model" data cube
Fold calculated images through instrumental parameters to obtain "observed" images
Compare model & observed images
Apply standard image reconstruction to obtain "clean image" data cube
Output 3D Model
Yes
OK
No

Non-thermal Gyrosynchrotron Emission

Strengths:

✓Diagnostic of magnetic fields in flares/CMEs

✓can be used to constrain fields of any strength (s >>1)

✓both optically thin and optically thick emission can be exploited

✓technique can be employed on the disk or above the limb

Weaknesses/complications:

✓Requires source modeling to disentangle electron energy distribution function from magnetic field

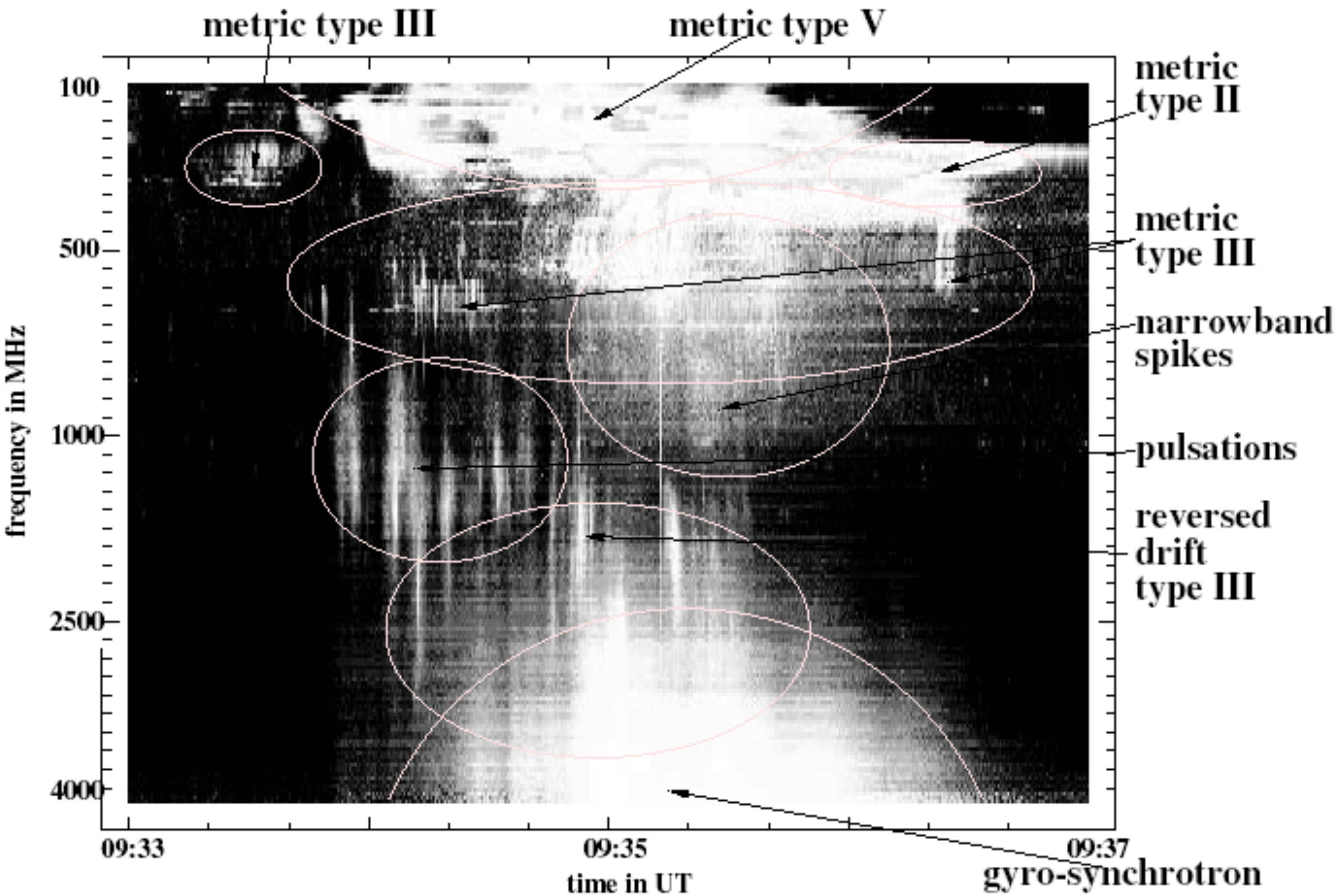

from Benz, 2004

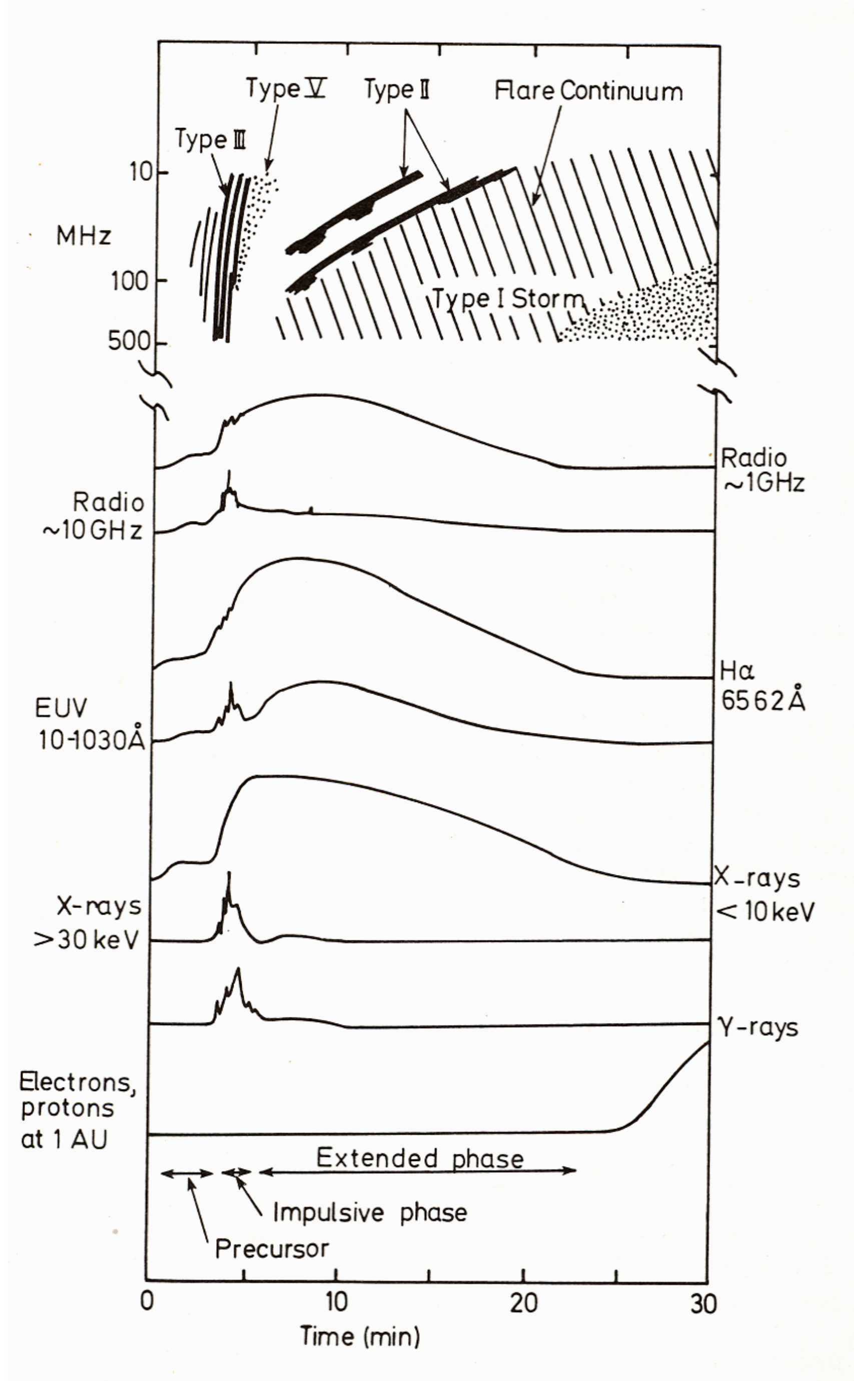

Type V
Type II
Flare Continuum
Type III
10
MHz
100
500
Type I Storm
Radio
~1GHz
Radio
~10 GHz
Hα
6562 Å
EUV
10-1030Å
X-rays
< 10 keV
X-rays
> 30 keV
γ-rays
Electrons,
protons
at 1 AU
Extended phase
Impulsive phase
Precursor
0
10
20
30
Time (min)

Dulk 1985

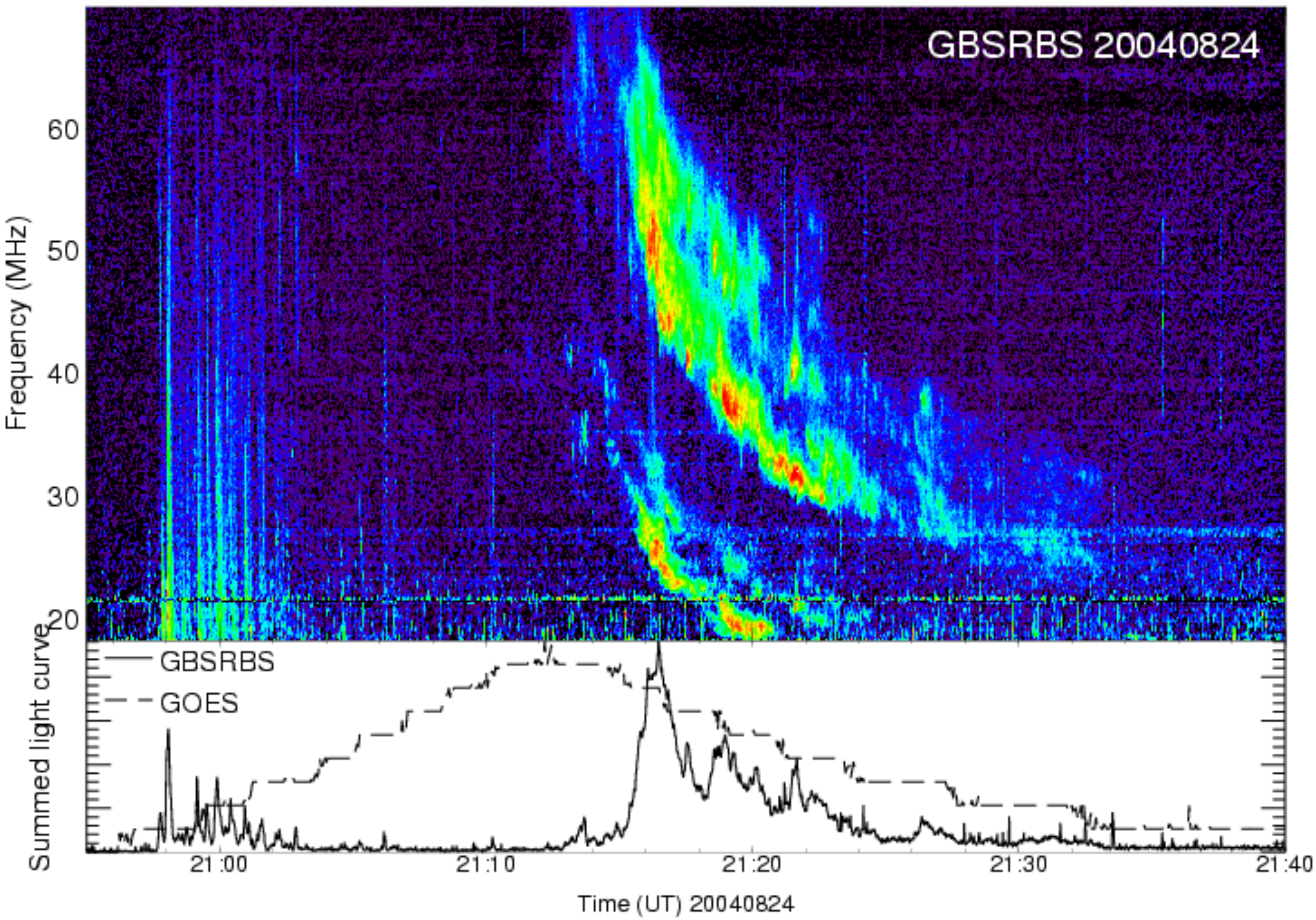

GBSRBS 20040824
Frequency (MHz)
60
50
40
30
20
GBSRBS
GOES
Summed light curve
21:00
21:10
21:20
21:30
21:40
Time (UT) 20040824

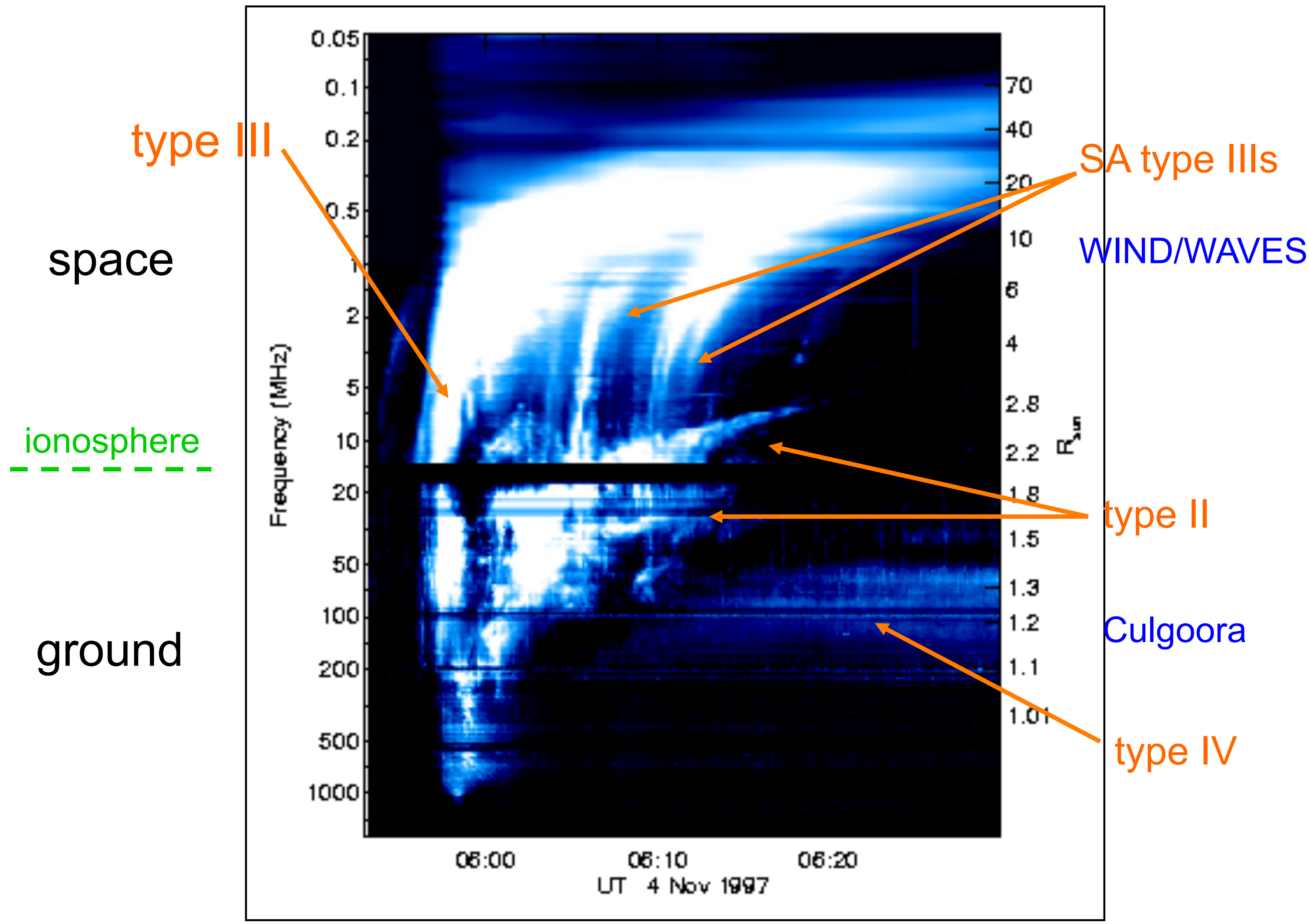

Dulk et al. 2001

Estimates of coronal magnetic fields using radio bursts

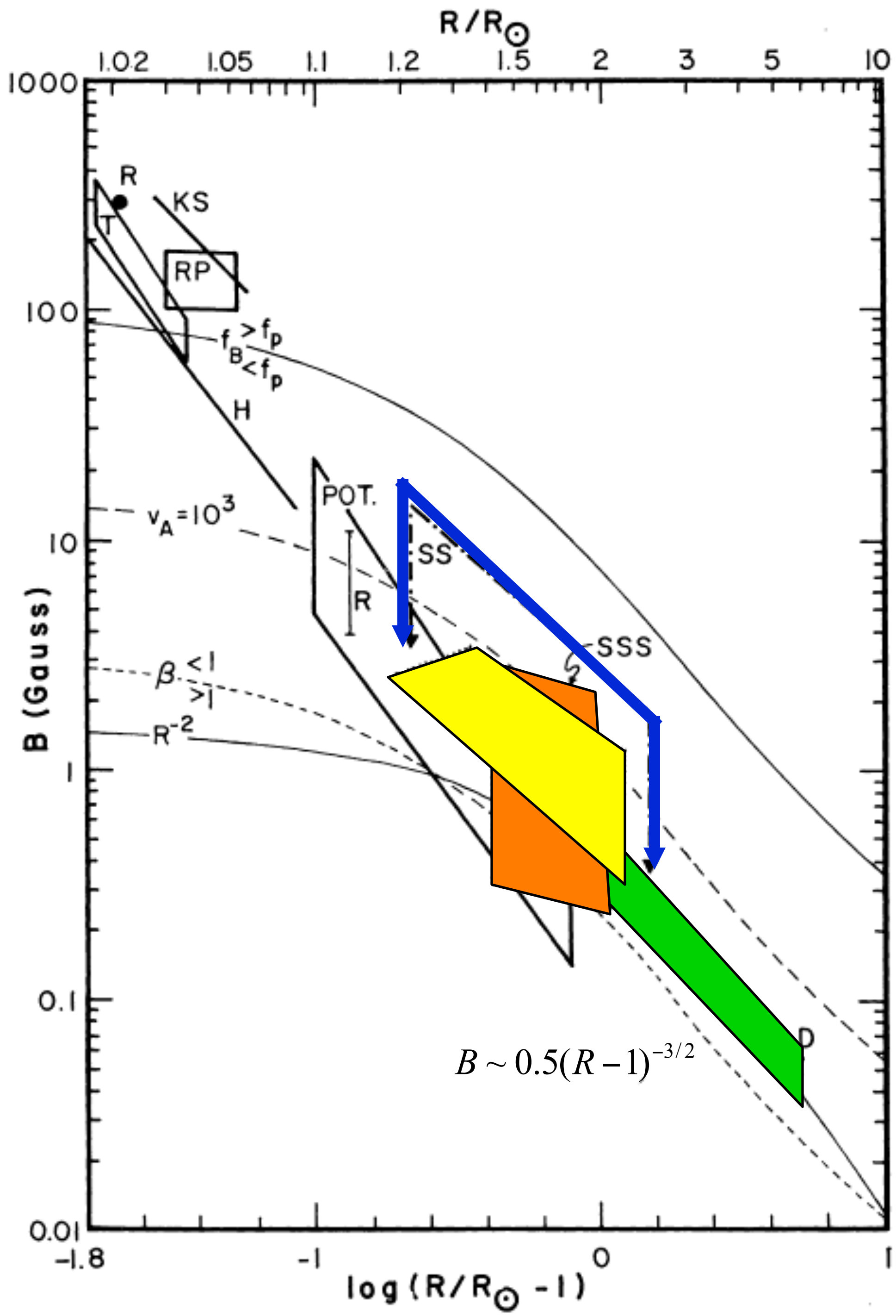

Type II bursts

Type III bursts

Type IV "slow drift continuum"

Dulk & McLean 1978

Very Large Array 5 November 2011

- D configuration
- 17 antennas
- 1-2 GHz
- 1024 channels
- Δt = 100 ms
- Dual polarization

An image is available for each integration time and frequency:

>20000 snapshots/sec !

A number of decimetric type III radio bursts (type IIIdm) were observed in association with an EUV jet observed by SDO/AIA.

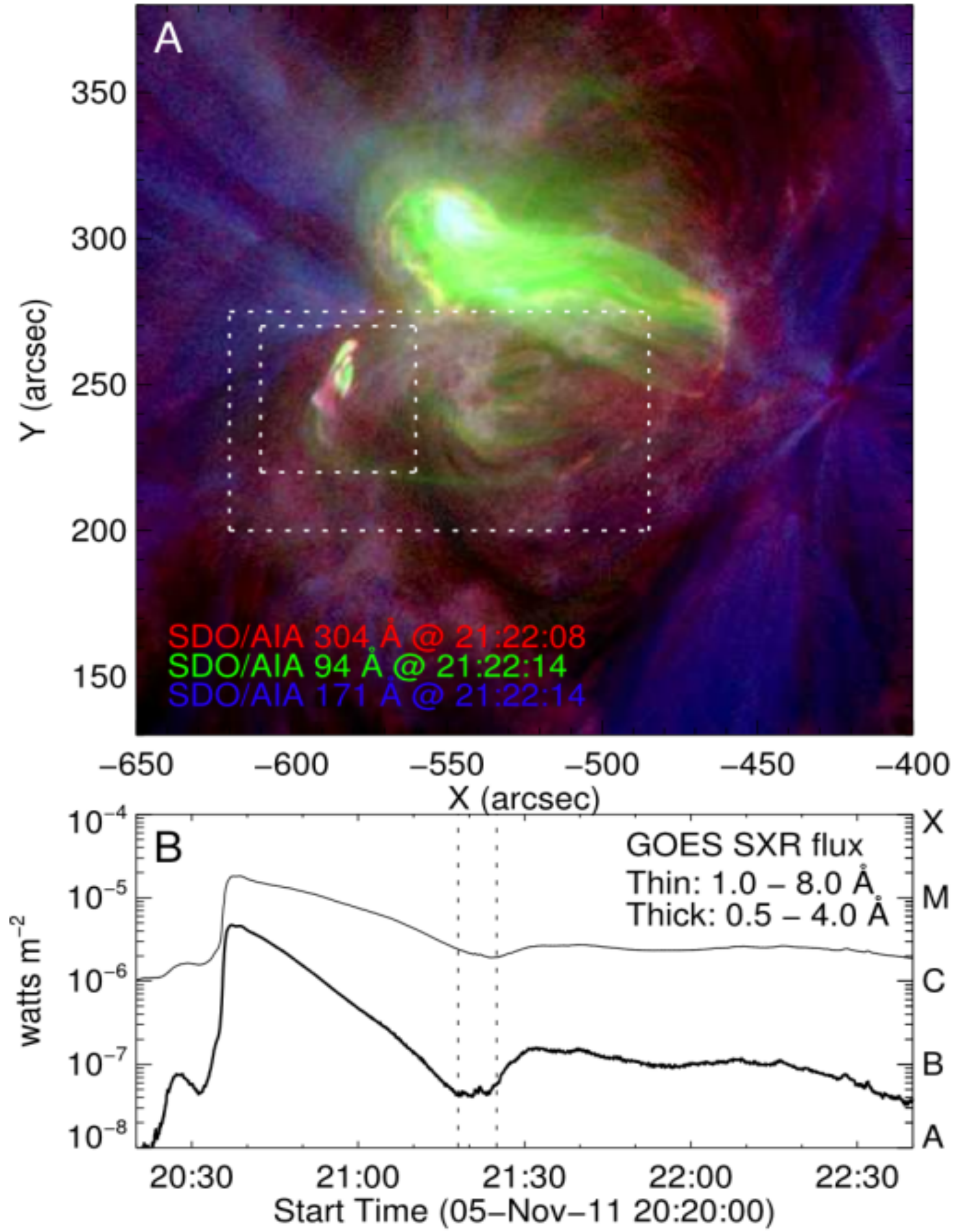

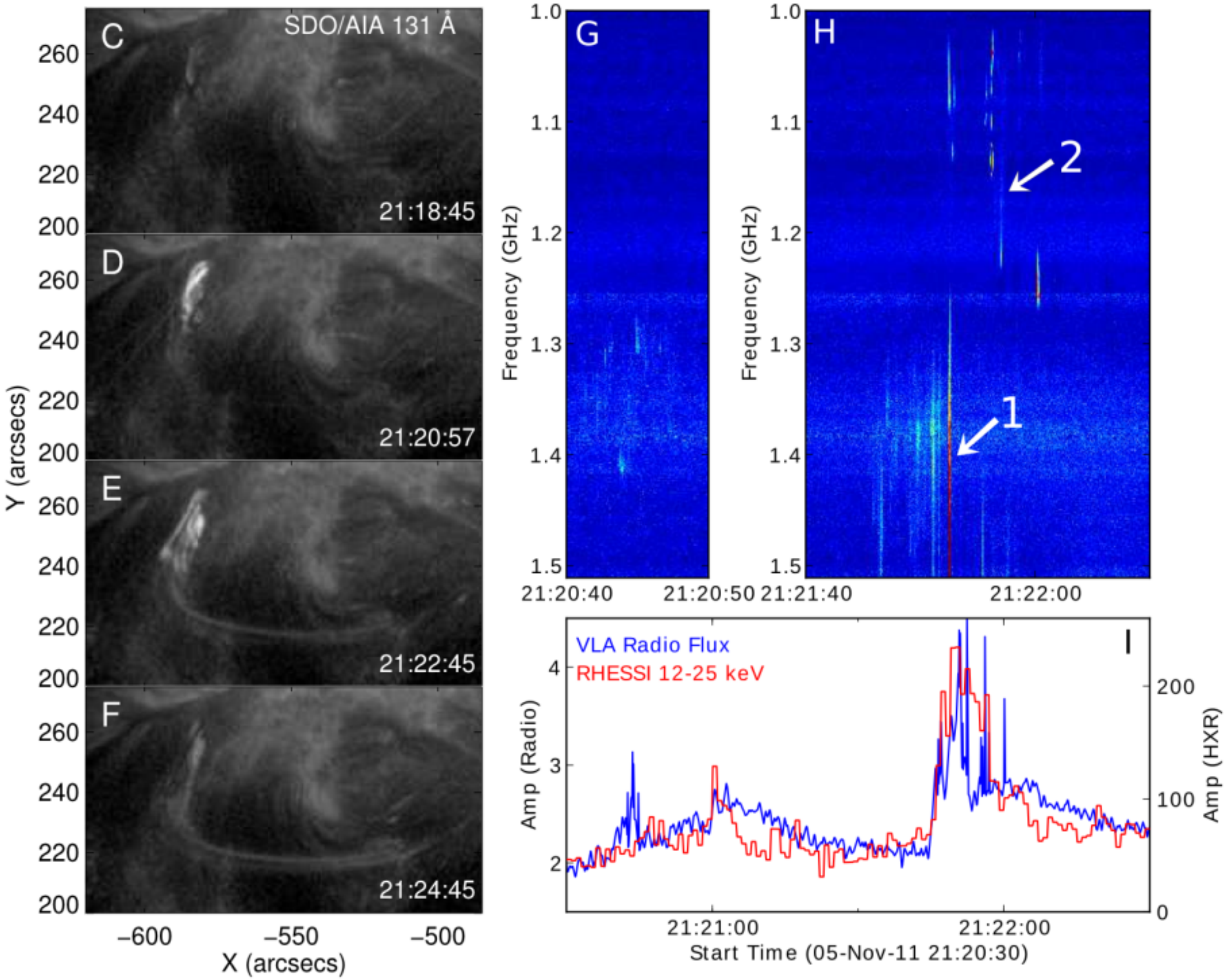

C
SDO/AIA 131 Å
21:18:45
D
21:20:57
E
21:22:45
F
21:24:45
Y (arcsecs)
X (arcsecs)
G
H
Frequency (GHz)
21:20:40
21:20:50
21:21:40
21:22:00
2
1
I
VLA Radio Flux
RHESSI 12-25 keV
Amp (Radio)
Amp (HXR)
21:21:00
21:22:00
Start Time (05-Nov-11 21:20:30)

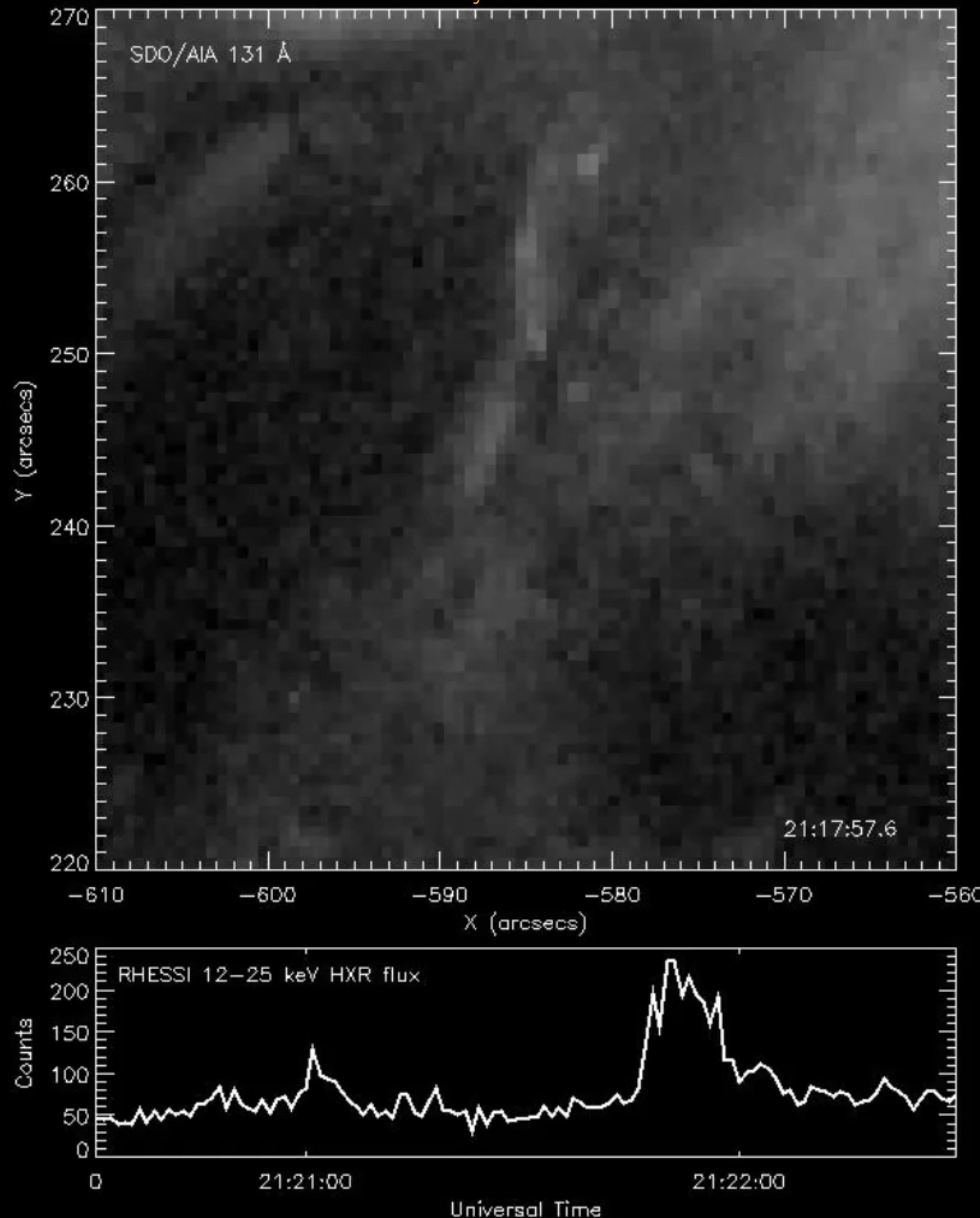
SDO/AIA 131 Å
21:17:57.6
Y (arcsecs)
X (arcsecs)
270
260
250
240
230
220
−610
−600
−590
−580
−570
−560
RHESSI 12−25 keV HXR flux
Counts
250
200
150
100
50
0
21:21:00
21:22:00
Universal Time

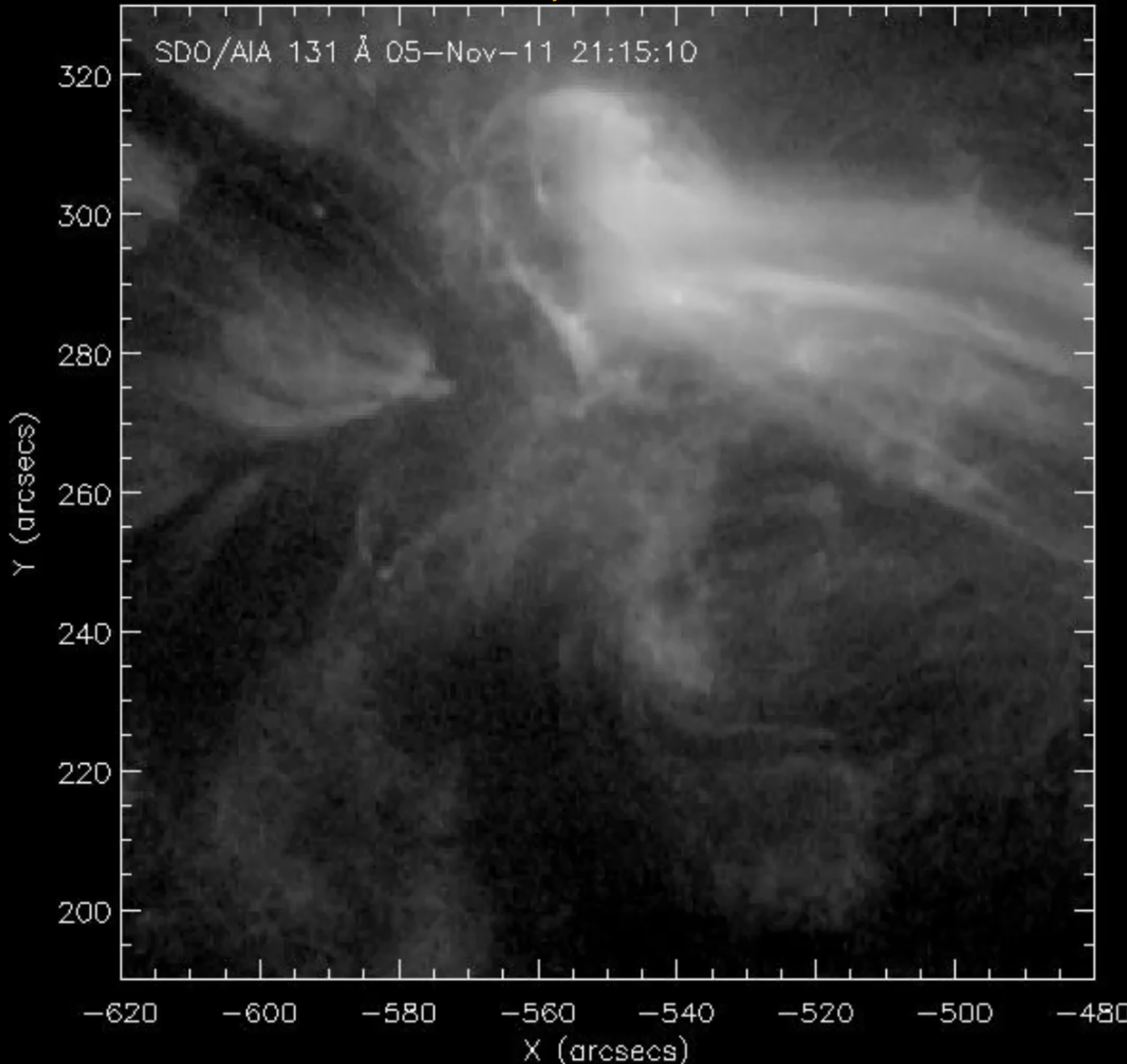
SDO/AIA 131 Å 05-Nov-11 21:15:10
320
300
280
260
240
220
200
Y (arcsecs)
-620
-600
-580
-560
-540
-520
-500
-480
X (arcsecs)

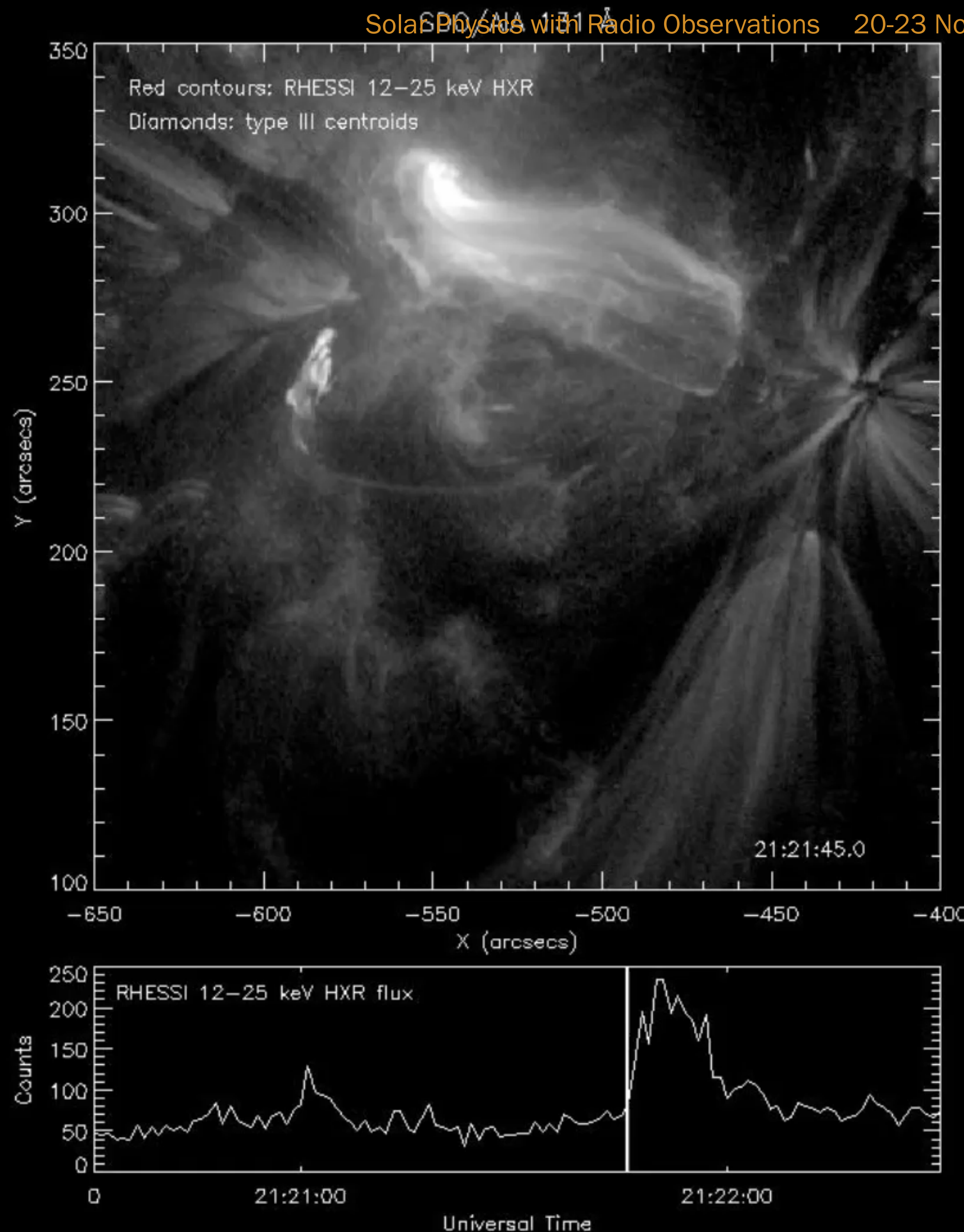
SDO/AIA 131 Å
Red contours: RHESSI 12–25 keV HXR
Diamonds: type III centroids
21:21:45.0
Y (arcsecs)
350
300
250
200
150
100
−650
−600
−550
−500
−450
−400
X (arcsecs)
RHESSI 12–25 keV HXR flux
Counts
250
200
150
100
50
0
0
21:21:00
21:22:00
Universal Time

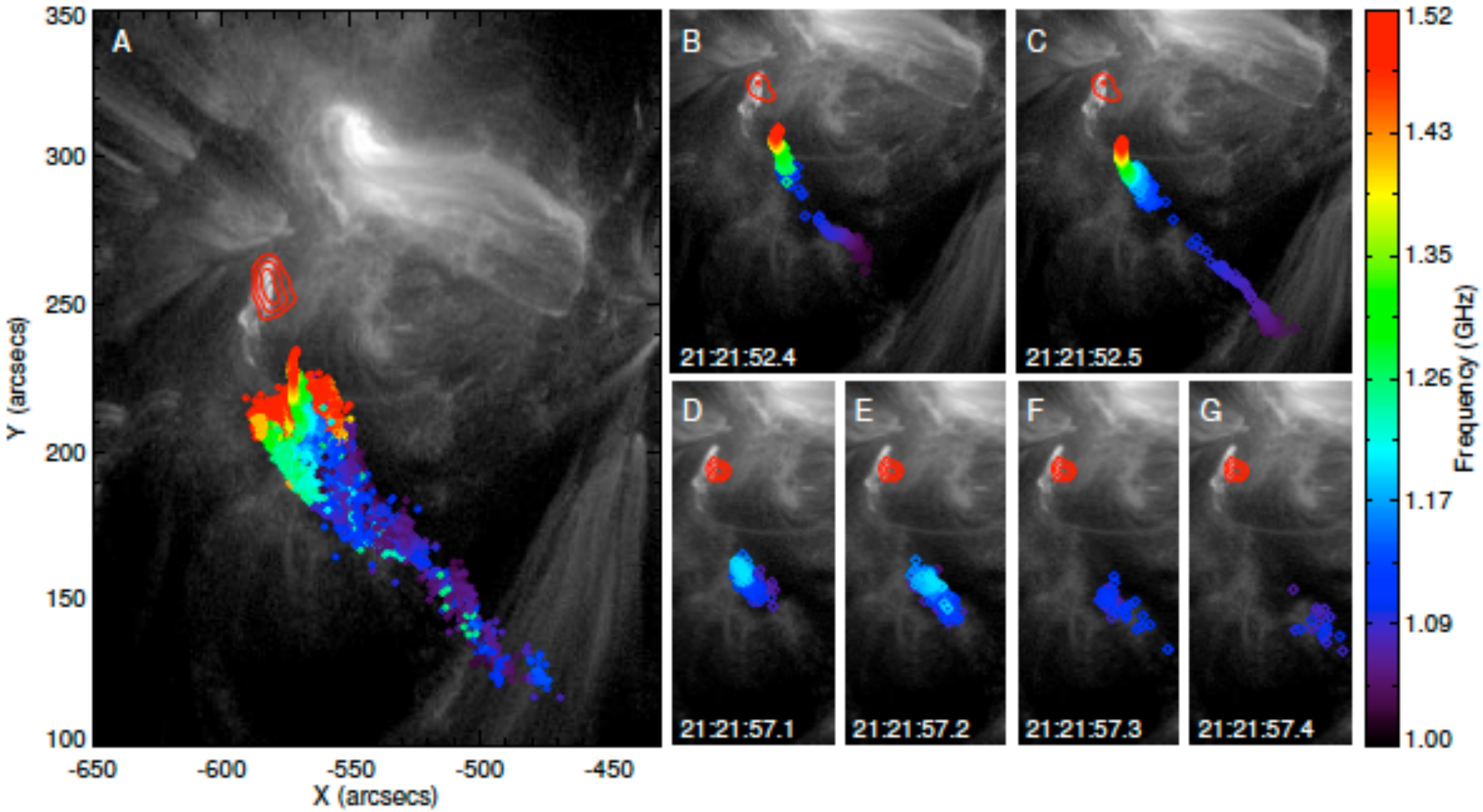

A
B
C
D
E
F
G
21:21:52.4
21:21:52.5
21:21:57.1
21:21:57.2
21:21:57.3
21:21:57.4
350
300
250
200
150
100
Y (arcsecs)
-650
-600
-550
-500
-450
X (arcsecs)
1.52
1.43
1.35
1.26
1.17
1.09
1.00
Frequency (GHz)

14 December 2006

X1.5 flare in AR 10930 at S06W46

The flare was accompanied by a fast CME and a particle event

AR 10930 was the site of an X3.4 flare the previous day

Both flares studied by Su et al. (2007) using Hinode data

Data used for this study:

- FST
- RSTN, GOES
- Hinode XRT & SOT/SP

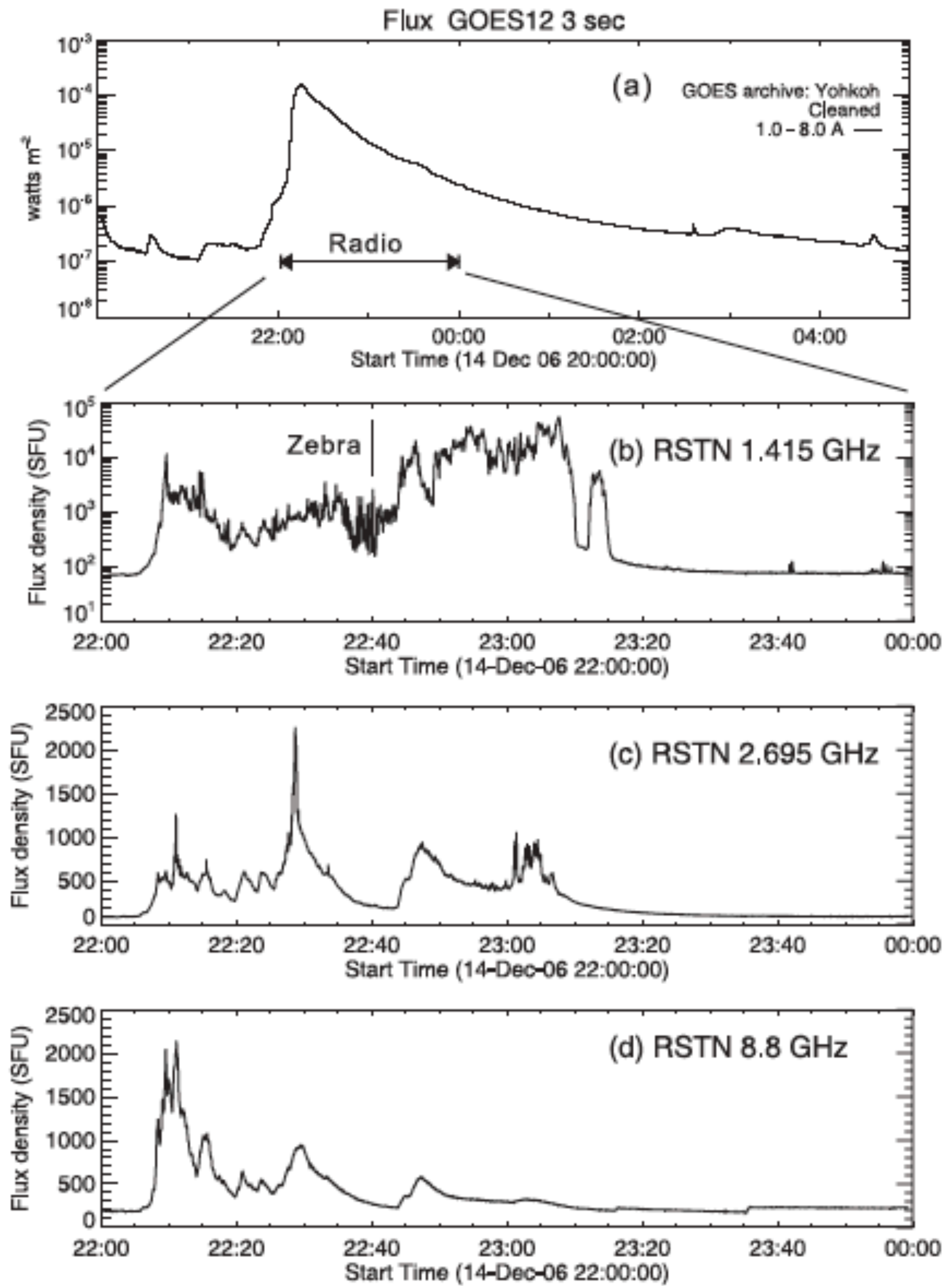

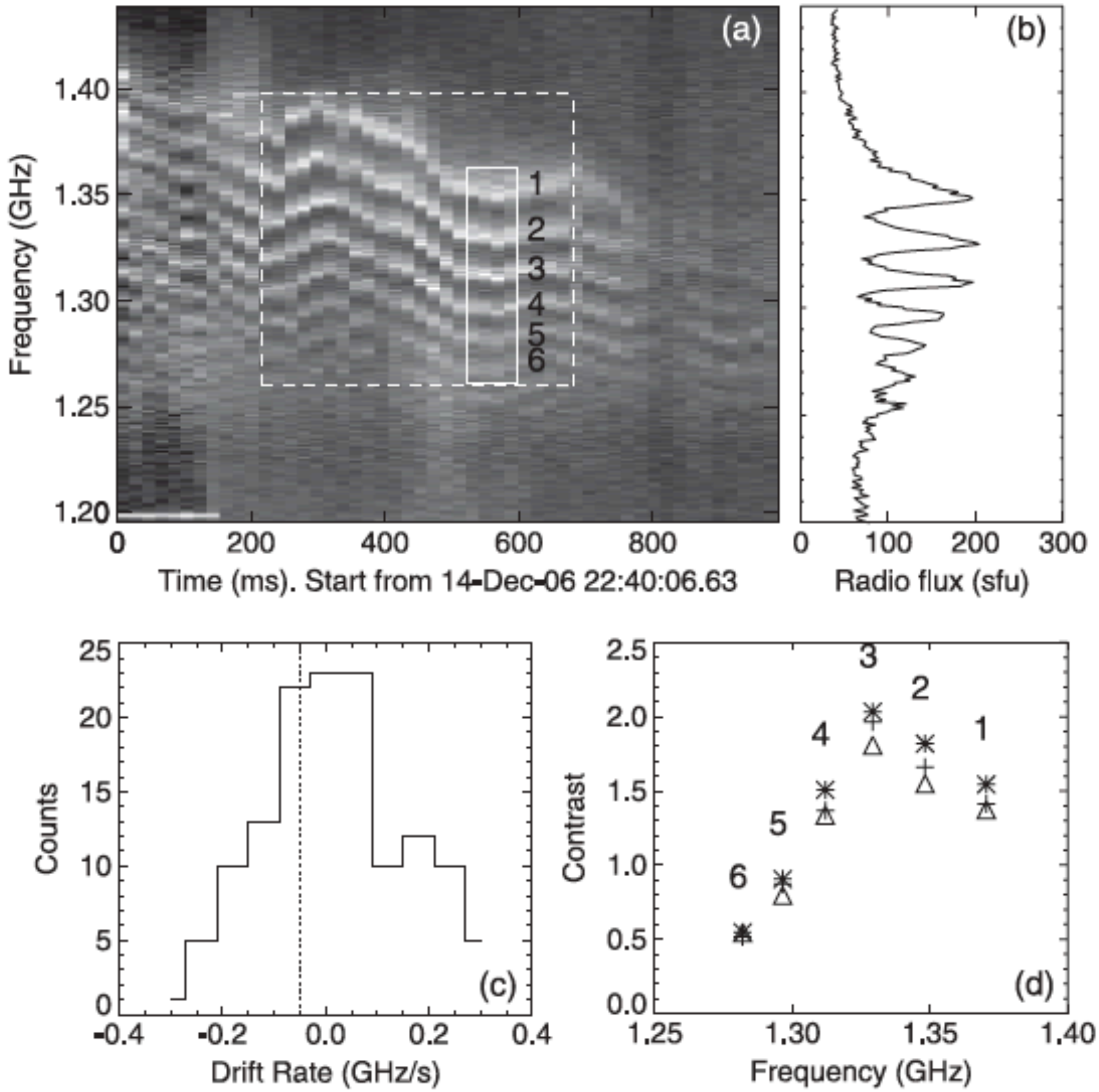
(a)
(b)
Frequency (GHz)
1.40
1.35
1.30
1.25
1.20
1
2
3
4
5
6
0
200
400
600
800
Time (ms). Start from 14-Dec-06 22:40:06.63
0
100
200
300
Radio flux (sfu)
Counts
25
20
15
10
5
0
(c)
-0.4
-0.2
0.0
0.2
0.4
Drift Rate (GHz/s)
Contrast
2.5
2.0
1.5
1.0
0.5
0.0
(d)
1.25
1.30
1.35
1.40
Frequency (GHz)

Double Plasma Resonance (DPR) model

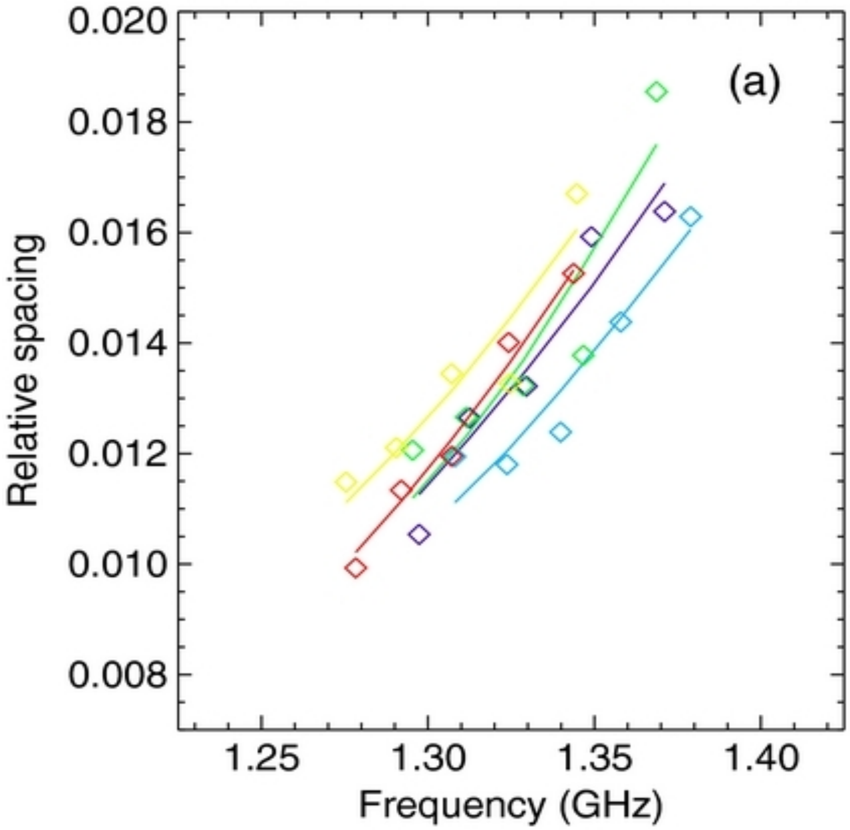

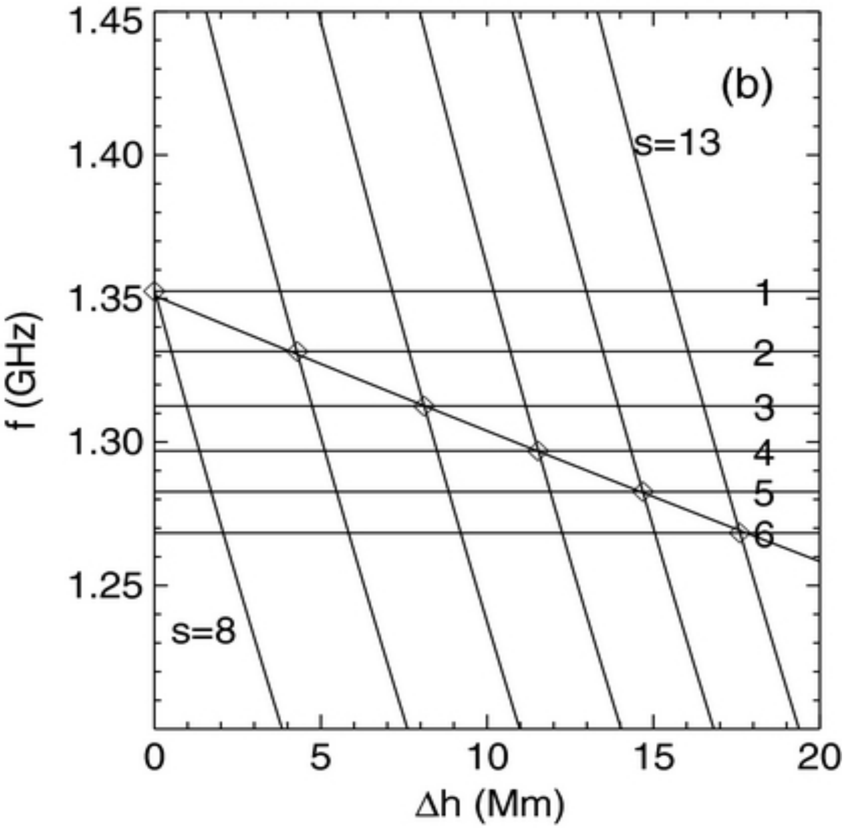

$$f = f_{UH} = (f_{pe}^2 + f_{ce}^2)^{1/2} = sf_{ce}$$

$$\approx f_{pe} \quad (f_{ce} << f_{pe})$$

$$f_{pe} = \left(\frac{e^2 n_e}{\pi m_e}\right)^{1/2} \quad \text{and} \quad f_{ce} = \frac{eB}{2\pi m_e c}$$

$$n_e = n_o e^{-\Delta h / L_n} \quad \text{and} \quad \mathrm{B} = \mathrm{B_o} e^{-\Delta h / L_B}$$

$$\left|\frac{\Delta f_s}{f_m}\right| \approx \frac{1}{s} \frac{1}{1 - (2L_n / L_B)}$$

NLFFF extrapolation performed by Ju Jing using SOT/SP data. Details given in the paper.

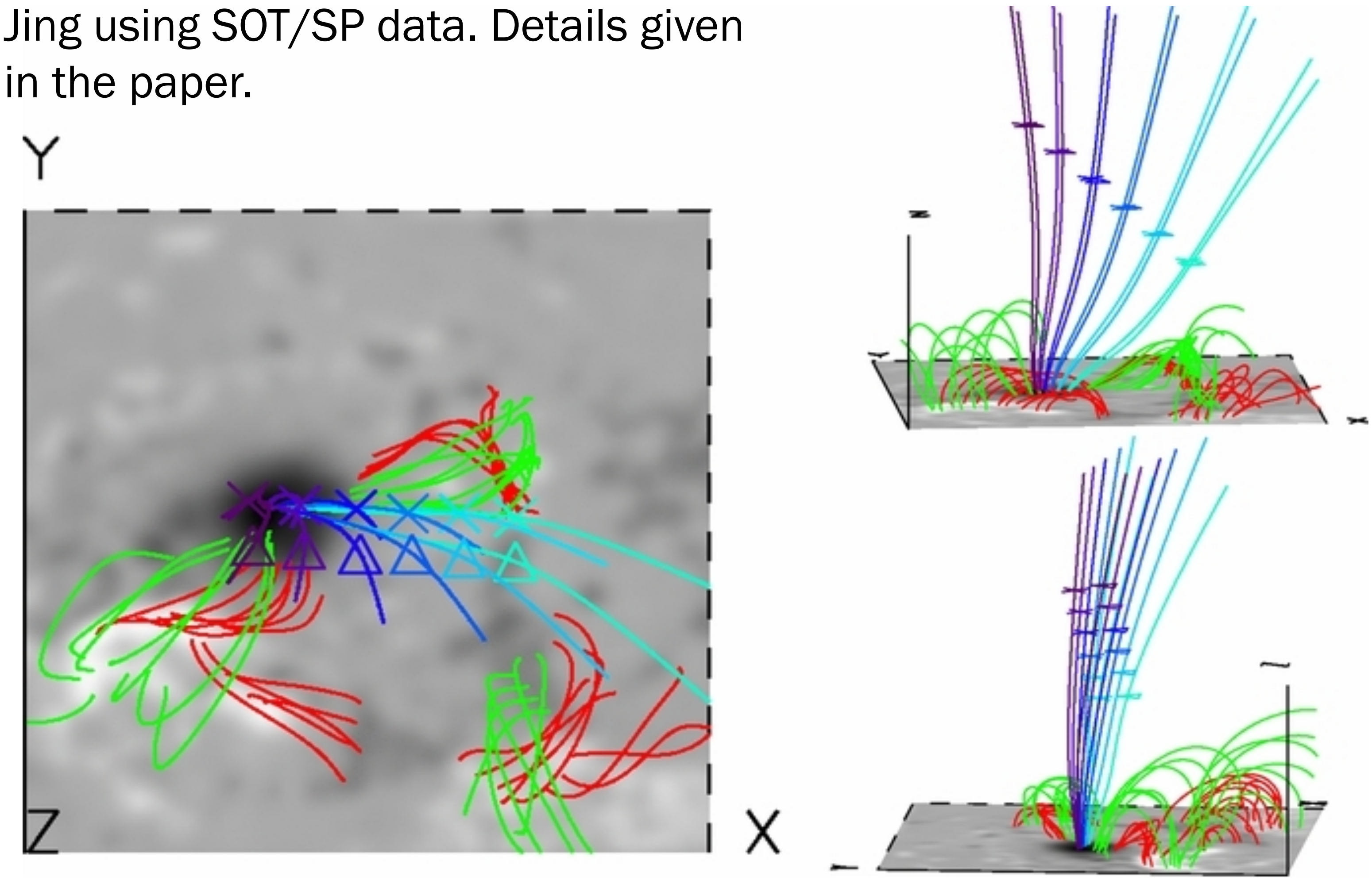

We are interested in constraining the source position within the 3D magnetic field. The “X” and triangle symbols denote possible de-projected positions of the continuum and zebra components, respectively.

RADIO BURSTS

Strengths:

✓Ubiquitous during flares (type IIIs)

✓can be used to constrain field connectivity/topology in energy release site (and in the wider corona!)

✓Can be used as probe of a large range of coronal heights

✓technique can be employed on the disk or the limb

Weaknesses/complications:

✓propagation issues

✓measurements specific to burst source regions